NEAREST NEIGHBOUR DEPENDENCE OF THE PRESSURE INDUCED PHASE TRANSITIONS OF $HgSe_x Te_{(1-x)}$

Basile Ghicopoulos

A THESIS

in the

Faculty of Engineering

Presented in partial fulfilment of the requirements for
the Degree of Master of Engineering at
Sir George Williams University
Montreal, Canada

August, 1973

NEAREST NEIGHBOUR DEPENDENCE OF THE PRESSURE INDUCED PHASE TRANSITIONS OF $HgSe_xTe_{(1-x)}$

BY

B. GHICOPOULOS

ABSTRACT

The rate of transition of $HgSe_xTe_{(1-x)}$ alloys under high pressure, has been investigated, by measuring the electrical resistance of the samples. The kinetics of these transitions are found to be of the first order type.

The transition pressures of $HgSe_xTe_{(1-x)}$ compounds and alloys have been calculated in terms of their lattice energies and their dependence on the nearest neighbour distance is analysed. The crystal structures are considered from the ionic character point of view. The variation of the atomic radii as well as other parmeters and quantities, is assumed to be proportional, throughout the calculations, with respect to the nearest neighbour distance.

The calculated transition pressure sequences is compared to the experimentally determined one (12). There is an excellent agreement between experimental and theoretical data, both confirming a linear trend. The attractive energy is shown to be dominant over the repulsive one, as expected, and the influence of the various parameters entering the energy equations, is discussed.

ACKNOWLEDGEMENTS

The author wishes to thank his research Supervisor, Dr. B. A. Lombos, for his continuous advice, interest and co operation during the course of the research of this work.

Thanks are also due to Mr. D. Lebidois and Mrs. A. Margittai of the Microelectronics Laboratory of SGWU, for their assistance in the experimental part.

TABLE OF CONTENTS

LIST OF FIGURES

LIST OF FIGURES

LIST OF TABLES

LIST OF TABLES

NOMENCLATURE

SYMBOL	DEFINITION
P	Pressure, (kg/cm^2)
V	Volume, (cm^3)
T	Temperature, (^oK)
G	Gibb's Free Energy, (ergs)
E	Lattice Energy, (ergs)
R	Resistance, (ohms)
k	Resistance Change per unit time (ohms/sec.)
α	Madelung's Constant
n	Repulsive Potential Constant
B	Repulsive Potential, (ergs)
e	Electronic Charge, Coulomb (cgs units)
C	Dipole-Dipole van der Waals Constant, ($ergs.cm^6$)
D	Dipole-Quadrupole van der Waals Constant, ($ergs.cm^8$)
r	Nearest Neighbour Distance, (A^o)
S'_6	Dipole-Dipole Sum Over the Odd Lattice Points of the Crystal, (cm)
S''_6	Dipole-Dipole Sum Over the Even Lattice Points of the Crystal, (cm)
c_{ij}	Dipole-Dipole Potential Constant of ion Combinations, (ergs)
S_8	Dipole-Quadrupole Sum Over the Odd Lattice Points of the Crystal, (cm)
S''_8	Dipole-Quadrupole Sum Over the Even Lattice Points of the Crystal, (cm)
U	Potential energy of the crystal, (ergs)

SYMBOL	DEFINITION
d_{ij}	Dipole-Quadrupole Potential Constant of ion Combinations, (ergs)
c'_{ij}	Repulsive Force Dependence on the Valence of the ions
b	Arbitrarily Chosen Constant, (ergs)
ρ	Empirically Adjusted Constant (A^o)
r_{ij}	Radius of Cation or Anion, (A^o)
v_{ij}	Valence of the First or Second ion
N_{ij}	Number of Electrons in Cation or Anion
M	Number of Unlike Neighbours in the Lattice
M'	Number of Like Neighbours in the Lattice
a'	Ratio of Like Over Unlike Neighbours
δ	Difference between ionic Radii, (A^o)
x_i, x_j	Electronegativities of atoms i and j respectively
r_{nij}	New Calculated Radii, (A^o)
r_{oij}	Originally Accepted Radii, (A^o)
I	Percent Amount of ionic Character, (%)
r_{jj}	Difference of Nearest Neighbours Distance between Se and Te, (A^o)
r_n	Calculated Value (new) of the Nearest Neighbour Distance, (A^o)
r_o	Originally Accepted Value of the Nearest Neighbour Distance, (A^o)
Δr	Difference of Nearest Neighbour Distance between HgSe and HgTe, (A^o)
V*	Volume of Activation, (cm^3/mole)
a	Lattice Parameter, (A^o)
c	Lattice Parameter, (A^o)
S	Entropy of the system, (cal deg^{-1})

PART I

THEORETICAL ASPECTS OF THE INVESTIGATION

1. GENERAL

1.1. Introduction

The application of high pressure to physical matter as a means of studying various chemical and physical phenomena, is considered to be of particular importance.

One such phenomenon is polymorphism, i.e. the transformation of substance, under pressure, from one phase to another. The pioneering work on the subject was carried out by P. Bridgman (1) and (2). Ever since, the interest on the subject and the related investigations have grown rapidly.

Of particular interest is the study of polymorphic transformations of solids when subjected to pressure. Again, Bridgman (3) has pioneered in this aspect. The approach taken was mainly from the thermodynamic point of view; conducting primarily volumetric measurements he determined the pressures at which transitions occured for the various solids under investigation. The various effects, due to pressure, on the transitions, are extensively discussed in (4). His study (5) of the velocity of the transitions, forms the basis for later studies.

In recent years, various investigators have reported either a reconfirmation of the results obtained by Bridgman for various substances, or an extension of those measurements to others. Thus, G. Kennedy and P. LaMori (7) determined the transition pressures for a wide range of compounds, C. Pistorius (8) reports same on alkali Bromides and Iodides, A. Jayaraman et

al (6) have investigated some II-VI compounds; B. Lombos et al (9) and (10) investigated the kinetic aspect of the transitions induced by high pressure; R. Jacobs (11) reported on the transition occurring in metallic halides.

Studying this last report in more detail, one observes that, the calculated, as well as the experimental, equilibrium pressures at which transformations occur, exhibit a linear dependency with respect to the inverse of the nearest neighbour distance (1/r). It is this particular observation which gave rise to the present work, as it is stated below.

The necessary theoretical background is presented in Part I, sections 2.1 (pressure induced phase transitions), and 2.2 (Kinetics of the polymorphic transition), while Section 2.3 deals with the detailed theoretical investigation of the nearest neighbour dependence of transitions in ionic crystals. The experimental investigation is outlined in Part II, Section 3, while the results are to be found in Section 4, the discussion and the conclusion in Section 5 of Part II. The calculation for the unit cell volumes are to be found in Appendix A. The computer programs used, with their flow charts and representative print-outs are included in the Appendices B and C.

1.2 Purpose of the Present Work

The purpose of the present work is twofold: First, it is the theoretical treatment of the nearest neighbour dependence of the pressure induced phase transitions of $HgSe_xTe_{(1-x)}$. Second, it is the experimental investigation of the kinetic aspect of the same.

The emphasis of this treatment is in the investigation of the 1/r dependence of the pressures at which transitions occur in the $HgSe_xTe_{(1-x)}$ compounds and their alloys. As it is mentioned previously, the work by R. Jacobs (11) in the alkali halides suggest a linear dependence. In the present theoretical treatment, we attempt to show that this basic assumption, i.e. linear dependence, is also true in the case of the $HgSe_xTe_{(1-x)}$ compounds and their alloys so that, the experimental data obtained in Microelectronics laboratory of SGWU (B. Lombos, (12)) can be interpreted. These data suggest a linear relationship of pressure vs. composition.

In addition, experiments were performed in order to determine the volume of activation for HgSe, HgTe compounds and their alloys so that, their kinetic aspect can be characterised.

2. ANALYSIS OF PRESSURE INDUCED SOLID-SOLID PHASE TRANSITIONS

2.1 Introduction

The thermodynamic parameters (pressure, volume, temperature) describing the state of a system, are related by the mathematical relationship,

$$f(P,V,T) = 0 \qquad (1)$$

which is known as the (general) equation of state of the system. This equation can be expressed in various other forms, depending on the nature of information desired. In general, though, for these equations to be determined experimentally all three variables must be measured at the same time so that, a PVT surface can be determined.

In his original investigations, Bridgman (1), (2) has observed that all substances, when subjected to pressure, undergo a transformation. This means that a liquid can change to solid or a gas to solid or, even from one phase of a solid to another (solid-solid). Of particular interest here is this last one, the solid-solid phase transformation. Many solids are known to have several stable phases at different pressures.

Each one of those phases will have its own equation of state. It is extremely difficult, if not impossible, to characterise the solid's behaviour by a simple equation in a certain P, T range.

Initially, attempts were made to specify the temperatures, as a function of pressure P at which transitions occured. However, extensive volumetric measurements have been performed on solids under pressure. The commonly utilised

experimental technique to make such volumetric measurements, is the one employing the piston-displacement in a pressure chamber principle. Such an arrangement is shown in Fig. (3-2). The obtained data permit both, the detection and the characterisation of the transition. When a discontinuity in volume, as a function of P, is observed, the transition is of 1st order. Otherwise it is of 2nd order. Latent heat may also be present (1st order) or not (2nd order).

The 1st order transitions are due to, primarily, change in the crystal structure. There are many such crystal forms known, existing primarily because of small differences in internal energy among them. R. Bradley (13) suggests that a combined approach, in terms of thermodynamic parameters and of Gibb's free energy, would be more beneficial in discussing this type of transition. He concludes that, since the slopes of the surfaces in the G, P, T diagram are such that,

$$-\left(\frac{\partial G_2}{\partial T}\right)_P > -\left(\frac{\partial G_1}{\partial T}\right)_P \qquad (2)$$

where the subscript 1 denotes the lower pressure phase and subscript 2 the higher pressure one, and since the higher enthalpy is above the transition point, the "second" phase, i.e. the one at high pressure, is the more stable one.

A phenomenon, associated with the solid-solid transition and being quite distinct, was observed by P. Bridgman (5). He found that, at the equilibrium pressure, many transitions

failed to materialize. In other words, even when the two phases were in contact with each other, the rate of transition would go to zero. He termed this as the "region of indifference". Since it has been determined that this phenomenon, usually, is not appearing due to equipment short comings, it must be concluded that it is something due to the transition itself. It is similar to the hysteresis effect. Many substances have their own "zone (region) of indifference", and its width is variable, depending on the substance.

Of importance, also, is the measurement of the rate at which a transition occurs. It has been found that this rate varies according to the direction in which the transition is running with the lower values (slow transition) in the direction of increased pressures. This sluggishness is also due to the reconstructive process which takes place, resulting in a new crystal structure at the high pressure phase.

In addition to volume discontinuity in the $HgSe_xTe_{(1-x)}$, a change of the electrical resistivity of the solid under pressure, due to electronic structure changes, occurs and it can be utilized as a means of detecting and studying a transition. The discontinuity of the resistance, at a particular pressure, is indicative of a 1st order phase transition, since it is related to the crystal structure.

These measurements can be performed with a normal piston displacement high pressure machine and a resistor bridge. Furthermore, they constitute a more precise technique of detecting the transition since the resistance variation is of the order of magnitude of 10^4, while the volume discontinuity is of the order of magnitude of 10^{-1}.

2.2 Polymorphic Transition Kinetics

The pressure induced phase transitions, as any physical or chemical reactions, proceed, from the low-pressure phase to the high-pressure one at specific rates. Owing to the nature of the phenomenon, the rate at which the transition proceeds cannot be measured directly. Various methods of indirect measurements are applied to study it.

The pioneer work, to determine the rate at which a phase transition proceeds under high pressure is due to P. Bridgman (5). Essentially, he measured the rate at which pressure could increase or decrease toward the equilibrium point, this rate actually being directly proportional to volume changes with the lower volume value at the high pressure phase. In addition, he has determined that, with increasing pressure, the rate of the reaction increased quite rapidly. Furthermore, as the pressure increases, there will be a specific range - "zone of indifference" - where the transition will not proceed, i.e. for all practical purposes its velocity will be zero.

An alternate method of measuring the rate of a transition in a semiconductor is by measuring the change of the electrical resistance of the material under study, at constant pressures and constant temperature. Here, a proportionality between resistance and phase change is assumed, as indicated by B. Lombos (10). Similar measurements of resistance change as a function of temperature, reported by A. Onodera (15), could also be utilized as a measure of the transition rate.

In the transition state method, as outlined by Evans and Polanyi (14) the following relationship is assumed to hold true:

$$\left(\frac{\partial \ln k}{\partial P}\right)_T = \frac{\Delta V}{RT} \qquad (3)$$

Where ΔV is the change in volume occurring from the initial state volume to the transition state volume; k is the reaction rate constant of the transition; R is the gas constant and T the temperature. The quantity ΔV, commonly known as V^*, is also called "volume of activation". If one defines k as the rate of change of the resistance with respect to time, characterizing the transition, that is

$$k = \frac{\Delta R}{\Delta t} \qquad (4)$$

then the "volume of activation", as defined above, at constant temperature, can easily be determined using equations (3) and (4). The "volume of activation" is a composite function, as determined by R. Hamman (16)

When such measurements are performed, as outlined above, the task of characterising the transition from its kinetics point of view, becomes less complicated. Thus, if the calculated data, follow a linear pattern and there is a lattice re-arrangement, from the low pressure phase to a higher packed one at the high pressure phase, then the transition is said to be of the 1st order. If there is no such change, with the lattice retaining its original features the transition is characterised as of higher order.

2.3 Transitions in Ionic Crystals - Nearest Neighbour Dependence

The approach taken so far to investigate the polymorphic transition was entirely thermodynamic. However, treating the subject in the light of additional information provided by modern theories related to matter, the interaction between atoms must be considered as well. This suggests a combined thermodynamic and atomic approach. In the latter there is a distinction as far as the nature of binding of the atoms is concerned.

Insulator and semiconductor crystals, in general, are categorized as ionic or covalent. Furthermore, since the present work is concerned with the $HgSe_xTe_{(1-x)}$ compounds and their alloys, which are of a mixed ionic and covalent bonding nature, it is essential to emphasize that, in the following the ionic aspect will be treated only, with the amount of ionic character to be determined later on.

In the subsequent theoretical treatment, an attempt will be made to show the nearest neighbour dependence of the theoretically calculated transition pressures at which these compounds and their alloys would exhibit polymorphic changes.

The total potential energy in ionic crystals, which consist of positive and negative ions, is mainly due to Coulombic interactions. The repulsive forces present are more effective at shorter interatomic distances. The expression characterising the potential energy U of a crystal whose neighbour atoms are at

distance r, in generalised form, is:

$$U(r) = -\frac{\alpha e^2}{r} + \frac{B}{r^n} \qquad (5)$$

where: α = Madelung's constant

n = Repulsive potential constant

B = Repulsive potential

e = Electronic charge

The curve representing equation (5) is as shown in Fig. 2-1. The effect of nearest neighbour distance r is apparent. The point on the graph at which U(r) = 0, i.e. when it is crossing the abscissa, denotes that the repulsive and attractive interatomic forces are equal. The general form of the binding energy curve for all solids is similar to the one shown in Fig. 2-1.

An extended expression of the potential energy of the crystal also called the lattice energy, in the ionic crystals, is provided by the Coulomb, the dipole-dipole, the dipole-quadrupole and the repulsion energies. This lattice energy, then, is expressed as:

$$E(r) = -\left(\frac{\alpha e^2}{r}\right) - \left(\frac{C}{r^6}\right) - \left(\frac{D}{r^8}\right) + B(r) \qquad (6)$$

where: C, D = Van der Waals constants

r = Nearest neighbour distance

The first three terms of eq. (6) represent the attractive potential whereas the last one represents the repulsive one. The model to be followed for the calculations of the

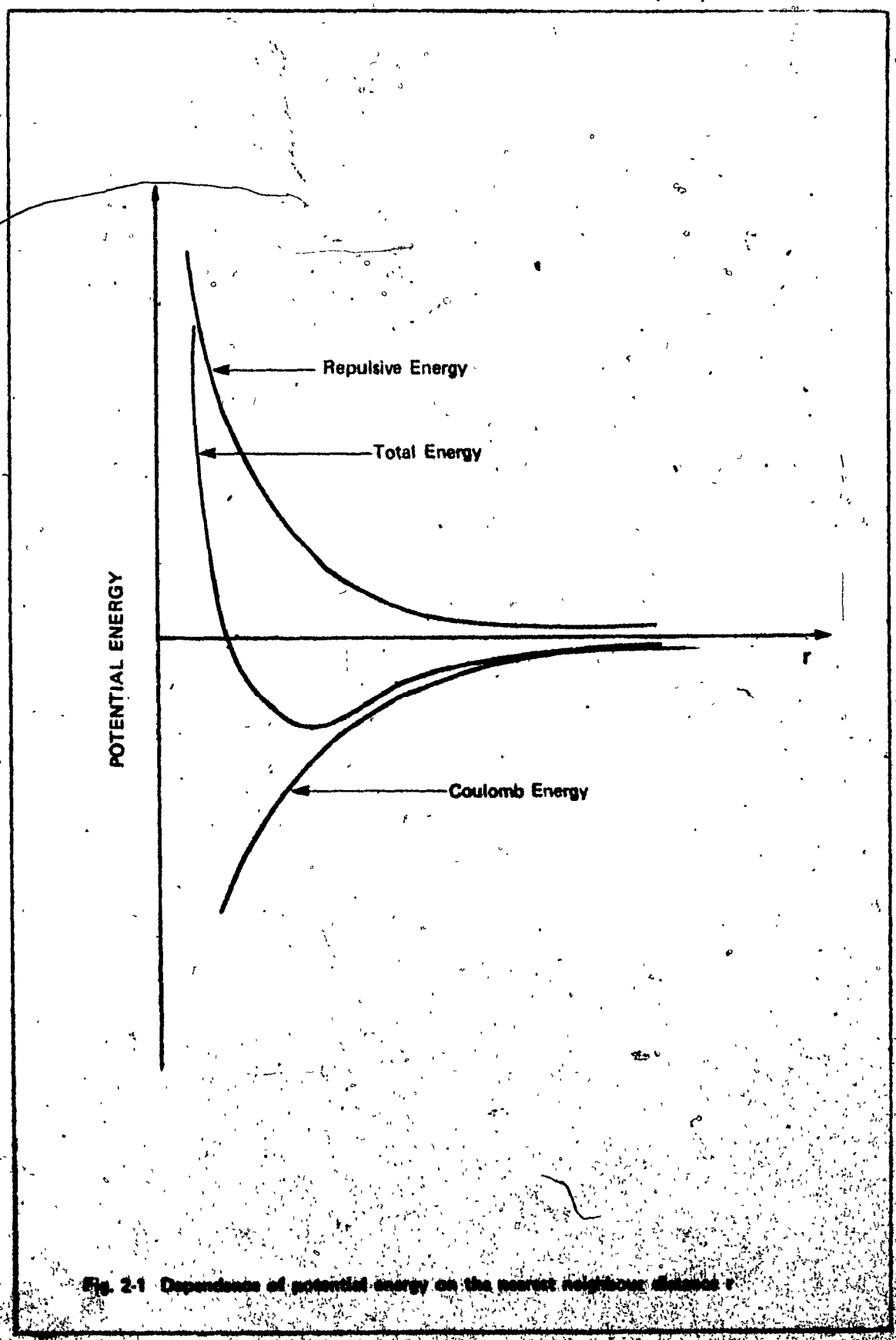

Fig. 2-1 Dependence of potential energy on the nearest neighbour distance r

lattice energies is the one for the alkali halides, as described by M. Huggins and J. Mayer (17). It is felt that, due to its ionic character considerations, its application to the determination of the lattice energies of the mercury chalcogenides, from the ionic point of view, is justified.

The individual terms then, of eq. (6) are analysed as follows:

(i) The Coulombic term $\left(\frac{\alpha e^2}{r}\right)$

where:

α = Madelung's constant

e = Electronic charge (in the C.G.S. Unit System)

r = Distance between nearest neighbours

The Madelung's constant is already known for some crystal structures. The distance r is provided either by published crystallographic data or calculated from the unit cell of the lattice modification in question.

(ii) In the dipole-dipole, $\frac{C}{r^6}$ and dipole-quadrupole, $\frac{D}{r^8}$ terms, C and D are the van der Waals constants and r is, again, the nearest neighbour distance. The van der Waals coefficients will be determined by the following equations as outlined by J. Mayer (18). Thus, the coefficient C will be given by:

$$C = S_6' c_{+-} + S_6'' \left(\frac{c_{++} + c_{--}}{2} \right) \qquad (7)$$

where:

S'_6 = The sum over the odd lattice points of the crystal.

S''_6 = The sum over the even lattice points of the crystal.

c_{+-} = Potential constant for a single charged positive and a single charged negative ion.

c_{++} = Potential constant for double charged positive ions.

c_{--} = Potential constant for double charged negative ions.

The coefficient D will be given by:

$$D = S'_8 d_{+-} + S''_8 \left(\frac{d_{++} + d_{--}}{2\sqrt{2}} \right) \qquad (8)$$

Where the individual quantities have the same meaning as in the eq. (7). The derivation of the dipole-dipole c_{ij} and dipole-quadrupole d_{ij} potential constants is outside the purpose of this work.

(iii) The repulsive energy term B(r).

The repulsive potential between two ions, is assumed to be given by the equation

$$B(r) = c'_{ij}\, be^{(r_i + r_j - r_{ij})/\rho} \qquad (9)$$

where:

ρ = Empirically determined constant

$b = 1 \times 10^{-12}$ erg (arbitrarily chosen)

r_i = Radius of the cation

r_j = Radius of the anion

The factor c'_{ij} determines the dependence of the repulsive force on the valence of the ions, which implies the actual charges of the ions. It is defined by L. Pauling (19) as follows:

$$c'_{ij} = 1 + \frac{v_i}{N_i} + \frac{v_j}{N_j} \qquad (10)$$

where:

v_i = Valence of the cation

v_j = Valence of the anion

N_i = Number of electrons in the cation

N_j = Number of electrons in the anion

Further, by substituting i and j with + and - respectively, to denote the nature of the ions, i.e. whether it is a cation or an anion, one may write:

$$c'_{+} = \frac{c'_{++}}{c'_{+-}} \text{ and } c'_{-} = \frac{c'_{--}}{c'_{+-}} \qquad (11)$$

In the present investigation, the correspondence is for:

c'_{+} = mercury and c'_{-} = chalcogenide

Their actual numerical calculation is as shown in the Appendix A.

The total repulsive energy term will be given by:

$$B(r) = B_{+-}(r) + \left[B_{--}(r) + B_{++}(r) \right] /2 \qquad (12)$$

where the individual terms are explained after equation (16). Considering the general expression of the repulsive potential between two ions, given by eq. (9) the individual terms of eq. (12) may be written as:

$$B_{+-}(r) = bc'_{+-} M e^{(r_+ + r_- - r)/\rho} \qquad (13)$$

and

$$\left[B_{--}(r) + B_{++}(r) \right] /2 = \left[bc'_{--} M' e^{(2r_- - a'r)/\rho} + bc'_{++} M' e^{(2r_+ - a'r)/\rho} \right] /2 \qquad (14)$$

Taking into consideration the relationships given by eq. (11) and the geometry of the lattice under consideration, eq. (14) can be expressed as:

$$\left[B_{--}(r) + B_{++}(r) \right] /2 = \left[bc'_{+-} M e^{(r_+ + r_- - r)/\rho} \right] \times \left[(S/a) e^{-(a'-1)r/\rho} \right] \qquad (15)$$

where:

$$S = \left(\frac{c'_{--}}{c'_{+-}}\right)\left(\frac{M'}{2M}\right)a'\left[1+\left(\frac{c'_{++}}{c'_{--}}\right)e^{-2\delta/\rho}\right]e^{\delta/\rho} \qquad (16)$$

The coefficients entering into equations (15) and (16) are:

b = The arbitrarily chosen constant as in eq. (9)

c'_{+-} = Dependence factor as calculated from eq. (10)

M = Number of unlike neighbours for the lattice under study

r_+ = Radius of the cation

r_- = Radius of the anion

r = Nearest neighbour distance

ρ = Empirically determined constant

$a' = \frac{\text{Distance between like neighbours}}{\text{Distance between unlike neighbours}}$ of the lattice in question

c'_{--} & c'_{++} = Factors as determined by eq. (7)

M' = Number of like neighbours for the lattice under study

δ = Difference between the ionic radii, r_+ and r_-.

The foregoing analysis has resulted in relationships which can be used to calculate the various forms of the crystal energy, taking into consideration the interatomic forces. The determined energy then is used to calculate the theoretical pressure of transition at which the low and high pressure modifications are at equilibrium. This implies that their thermodynamic potentials should be equal. In other words, using normal thermodynamic notation:

$$U_1 - TS_1 + PV_1 = U_2 - TS_2 + PV_2 \qquad (17)$$

where the subscript 1 denotes the low pressure phase and 2 the high pressure one. By neglecting the temperature terms, as suggested by R. Jacobs (11) and substituting U with the lattice energies $E_1(r)$ and $E_2(r)$ respectively, equation (17) can be solved for the equilibrium pressure P, or:

$$P \approx \frac{E_2(r) - E_1(r)}{V_1 - V_2} \qquad (18)$$

where V_1 and V_2 are the molecular volumes at the two phases.

The same procedure, as outlined above, is followed for the calculation of the energies at both the low and high pressure phases, noting that some numerical values of the various coefficients must be changed. This is due to the transformation of the lattice structure. Thus the alkali halides, for example, exist in two cubic crystal forms: At the lower pressures they exhibit the sodium chloride (NaCl) form (face-centered cubic) whereas at the higher pressures, the Cesium chloride (CsCl) form (body-centered cubic). These crystal structures are shown in Fig. 2-2 (a) and (b) respectively.

The mercury chalcogenides, and in particular HgSe and HgTe, exhibit, as it is found by Mariano and Warekois (20), the

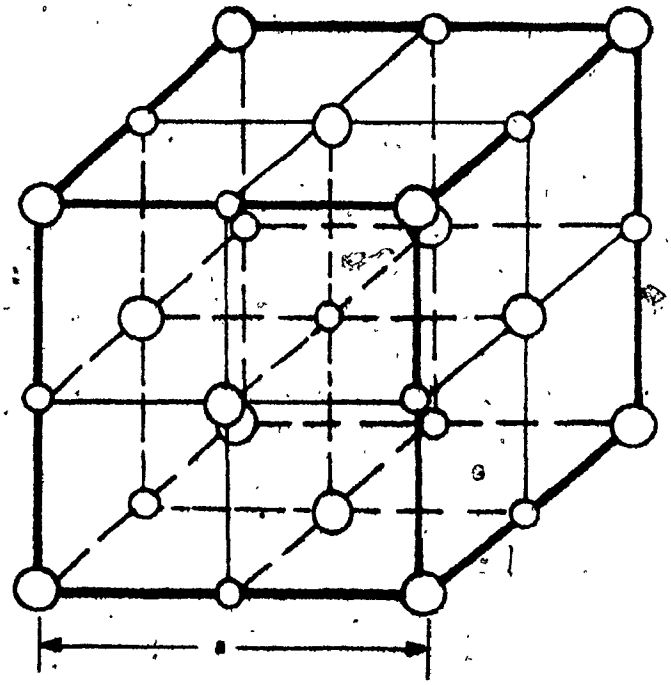

(a)

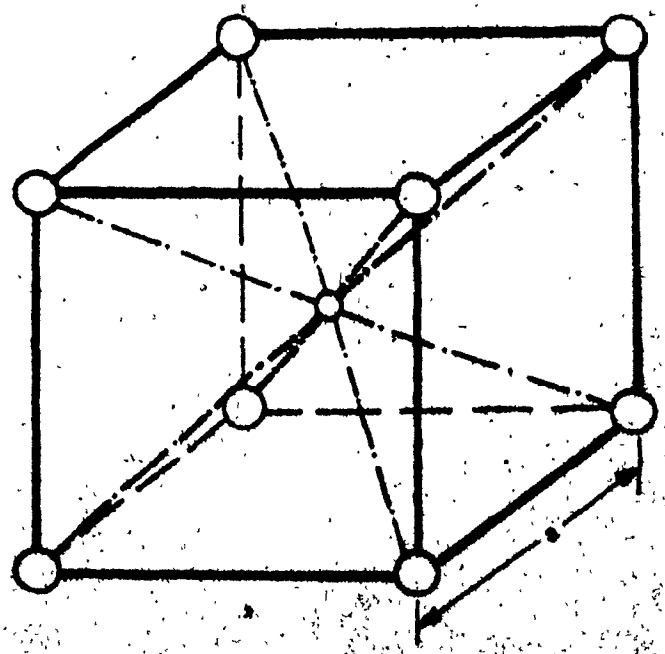

(b)

Fig. 2-2 Lattice structure, (a) NaCl, (b) CsCl

sphalerite (ZnS) form (cubic Zinc blende) at the lower pressures and that of cinnabar (HgS) form (hexagonal type) at the higher pressures. These structure forms are shown in Fig. 2-3 (a) and (b) respectively. Actually, the cinnabar lattice may be regarded as a strongly distorted sodium chloride type structure. The molecular volumes V_1 and V_2 are to be regarded as the "unit cell volume per atom" of the lattice in question, taking into consideration its geometry. The derived equations for the four mentioned types are to be found in Appendix A.

At the beginning of this section, it was mentioned that, the $HgSe_xTe_{(1-x)}$ compounds and their alloys are of a mixed bonding nature. Since this analysis is based on the ionic character of bonding, which is the case of interest here for these compounds, the degree of this partial ionic character has to be determined. Thus, the percent amount of ionic character I of a particular bond between atoms i and j will be given, as proposed by L. Pauling (21), by the equation:

$$I = 1-e^{-\frac{1}{4}(x_i-x_j)} \qquad (19)$$

where x_i and x_j are the electronegativities of atoms i and j respectively. The actual numerical values are to be found in Table VIII. The calculated amount of ionicity, then, is the quantity by which the tetrahedral radii for mercury, selenide, and telluride will be reduced. The resulting radii values are used for the calculation of the lattice energy, as outlined above.

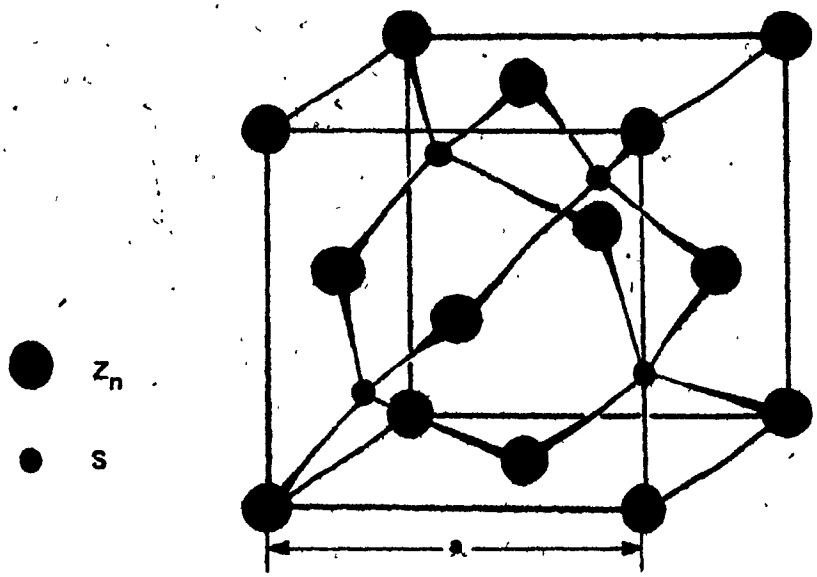

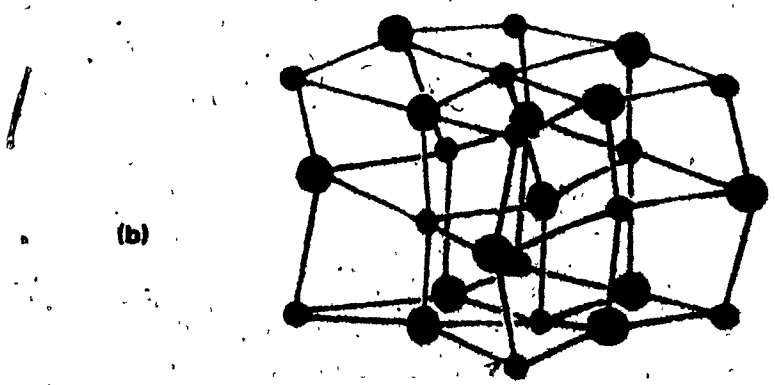

Fig. 2-3 Lattice structures: (a) Sphalerite, (b) Cinnabar (distorted NaCl)

The composition of $HgSe_xTe_{(1-x)}$ is taken on a proportional basis of the x value, starting with x = 1. Thus, the result is a gradual change in composition from one compound (HgSe) through its alloys with telluride, to the next compound (HgTe). The amount of change, now, of the radii which correspond to the alloys, is taken proportional to the original values. The respective r^+ and r^- radii, corresponding to the $HgSe_xTe_{(1-x)}$ compounds and alloys, will be determined by the following method:

$$\text{Let} \quad r^+ \equiv r_i \quad \text{and} \quad r^- \equiv r_j$$

then the new r^+ value is calculated by using the equation,

$$r_{ni} = (r_{oi} - I) \qquad (20)$$

where:

r_{ni} = New calculated r^+ radius

r_{oi} = Originally accepted r^+ radius

I = Percent amount of ionicity

The new r_- values will be given by the equation:

$$r_{nj} = (r_{oj} - I) + \left[(1-x)100\right](\Delta r_{jj} - I) \qquad (21)$$

where:

x = 1,0.8,0.6,0.4,0.2,0

r_{nj} = New calculated r^- radius

r_{no} = Originally accepted r^- radius

I = Percent amount of ionicity

Δr_{jj} = Se nearest unlike neighbour distance - Te nearest unlike neighbour distance

Similarly, the nearest neighbour distance r as determined by the lattice geometry, will be proportionally increased by the respective percent amount as one proceeds from HgSe to HgTe. This new value of r for each of the alloys, will be calculated from the equation:

$$r_n = r_o + \left[(1-x)100\right]\Delta r \qquad (22)$$

where:

r_n = New value of the nearest neighbour distance

r_o = Originally accepted value of nearest neig. dist.

x = 1, 0.8,0.6,0.4,0.2,0

Δr = HgTe nearest neighbour distance - HgSe nearest neighbour distance

The numerical values for the above quantities are shown in Table V. The "proportional change" approach is kept throughout the calculations of the molecular volumes as well, by considering the lattice parameter change from HgSe to HgTe.

PART II

EXPERIMENTAL PROCEDURES

3. METHODS

3.1 High Pressure Apparatus - General

The measurements made during the present investigation were mainly directed towards obtaining data for determining the kinetics of the phase transitions and the "volume of activation" for the various $HgSe_xTe_{(1-x)}$ compounds and their alloys.

The apparatus layout for carrying out these measurements is as shown in Fig. 3-2. A hydraulic system, which is activated by a low pressure pump, was used to generate the required high pressure. This is essentially achieved by a piston moving into a cylinder containing the sample under study. In order to achieve an equally distributed pressure on the solid sample under investigation, a fluid mixture of n-pentane - isopentane (in equal parts of 50% by volume) was used so that, a hydrostatic environment is created, meaning that no shearing components of the present forces are applied to the solid sample. The cylinder is made of three different layers of especially treated steel so that, it can withstand, from the elastic limit point of view, the pressures generated within it. A diagramatic representation of this apparatus is shown in Fig. 3-2. The piston used is made also of steel and a set of rings is used for ensuring no-leakage of the fluid contained in the cylinder. The arrangement is shown in Fig. 3-3 (a).

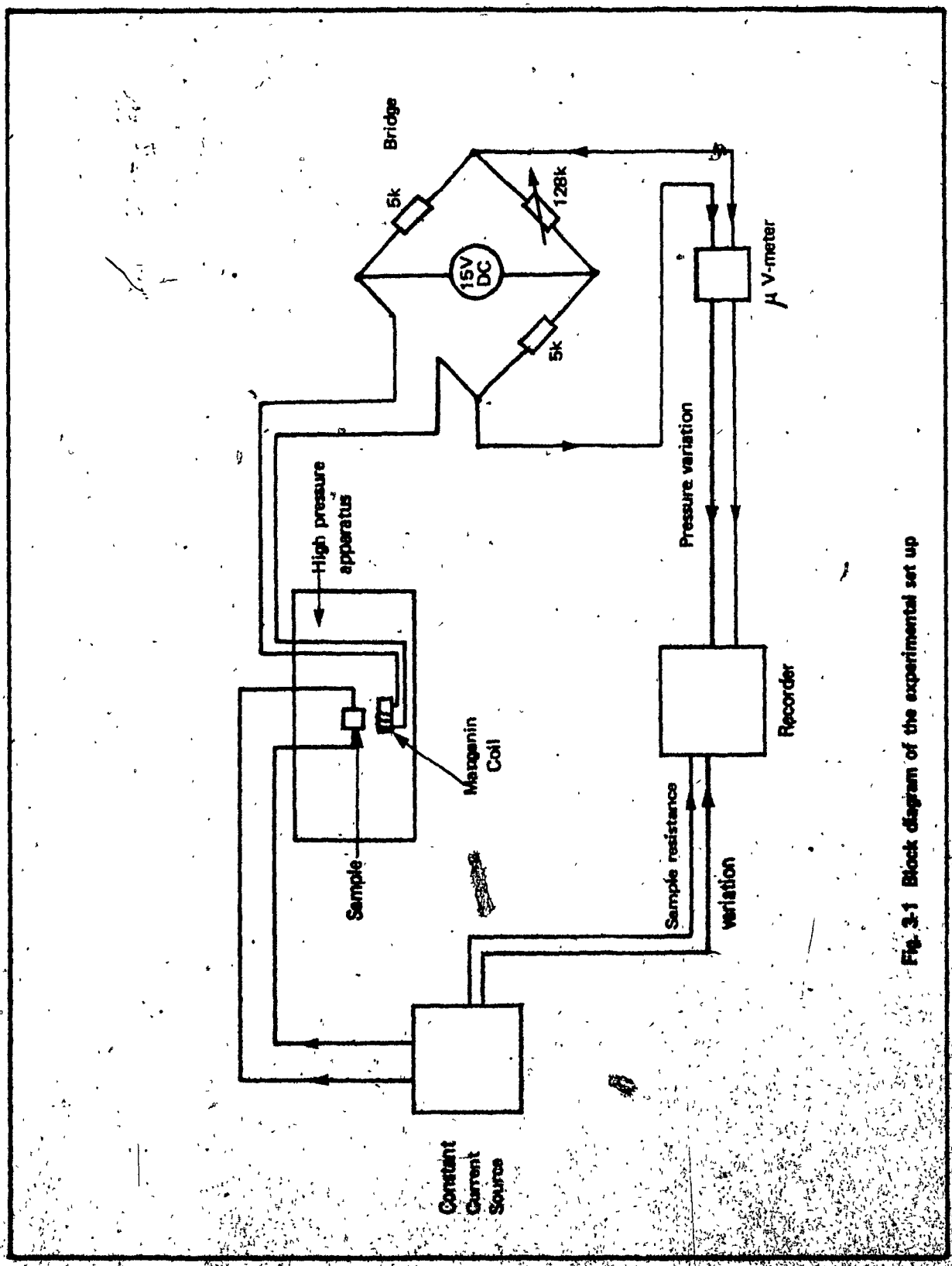

Fig. 3-1 Block diagram of the experimental set up

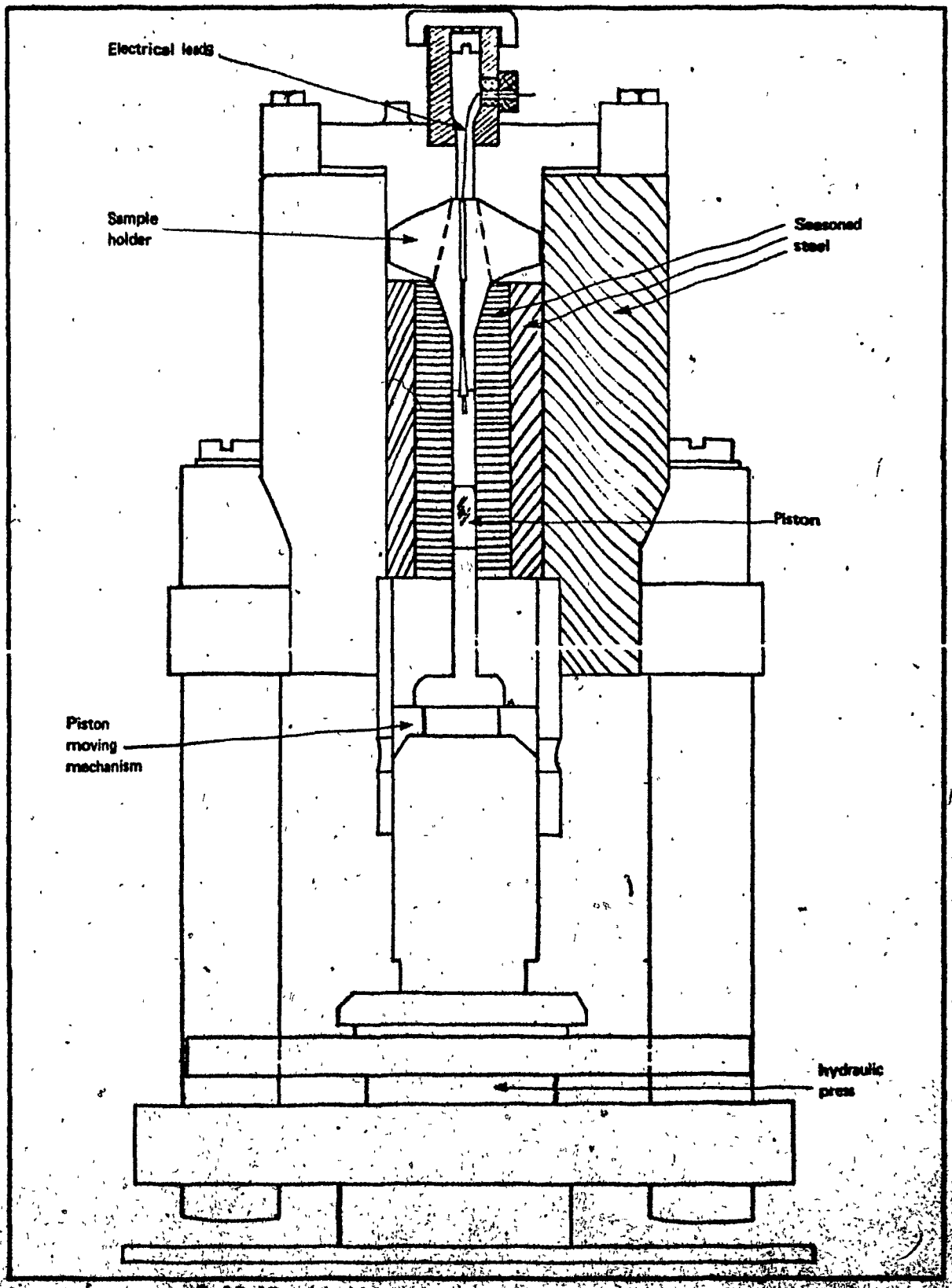

Fig. 3-2 View of the high pressure apparatus

3.2 High-Pressure Measurements

The generated high pressure is measured through the variation of the resistance of a manganin coil since its resistivity increases linearly with pressure. The electrical leads required for the monitoring of the resistance variation of the samples, are fed through the "sample-holder" arrangement as shown in Fig. 3-4. This arrangement, again, must ensure no leakage of the cylinder content. This is achieved by using a similar set, to those used with the piston, rings as shown in Fig. 3-3 (b).

The resistance change of a sample being connected to a constant current source, was monitored on a strip chart recorder running at constant speed. Similarly, on the same recorder, the pressure change, through an electrical bridge, was monitored. The samples used were provided by the Micro electronics laboratory of SGWU. The experimental set up is as shown in fig. 3-1.

The change of the electrical resistance of the sample as a function of time at constant pressure and temperature, is used to determine the kinetics of the transition. Similarly, the rate of the resistance change, as a function of pressure, at constant temperature, was used to determine the "volume of activation".

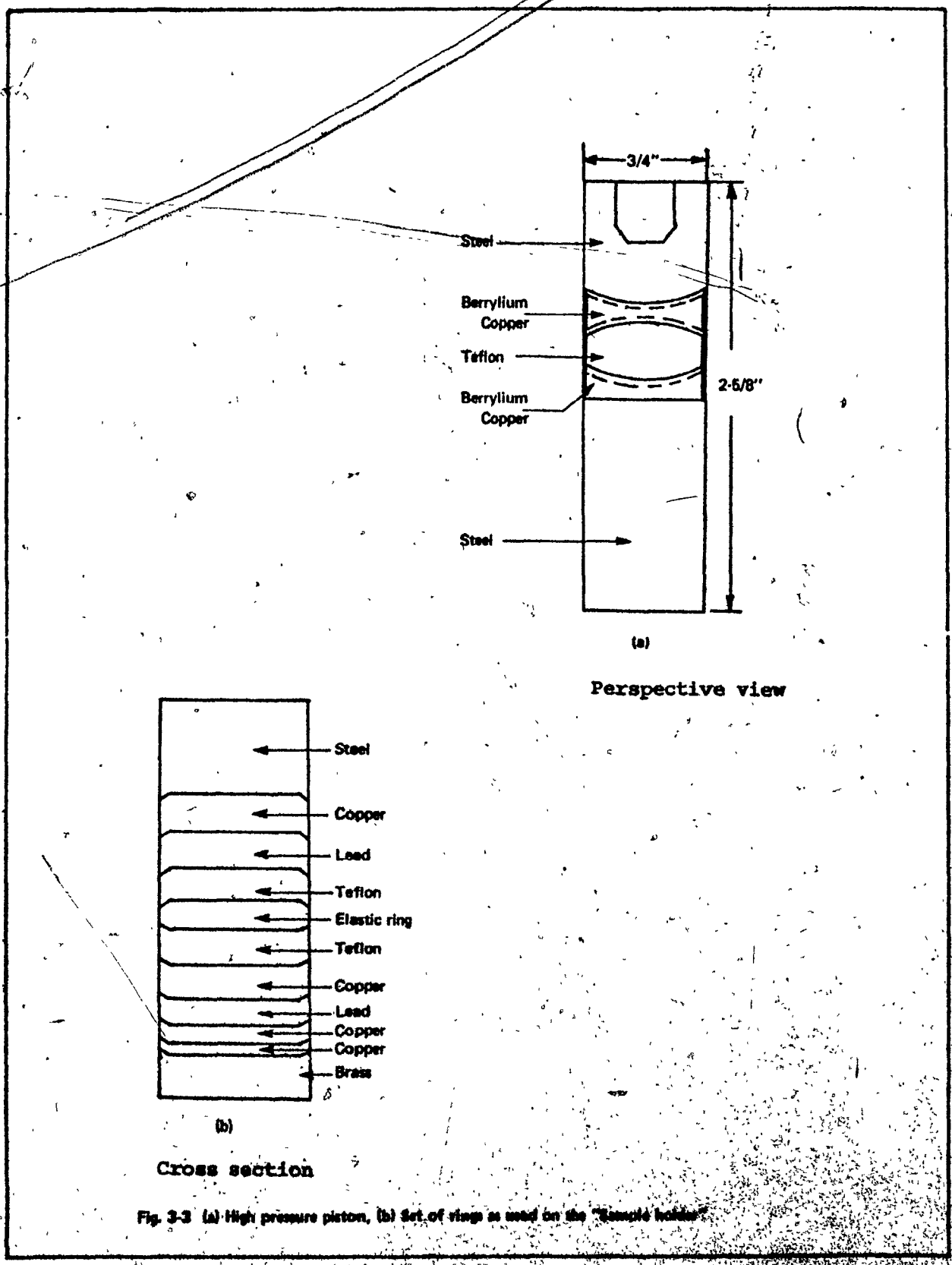

Fig. 3-3 (a) High pressure piston, (b) Set of rings as used on the "Sample holder"

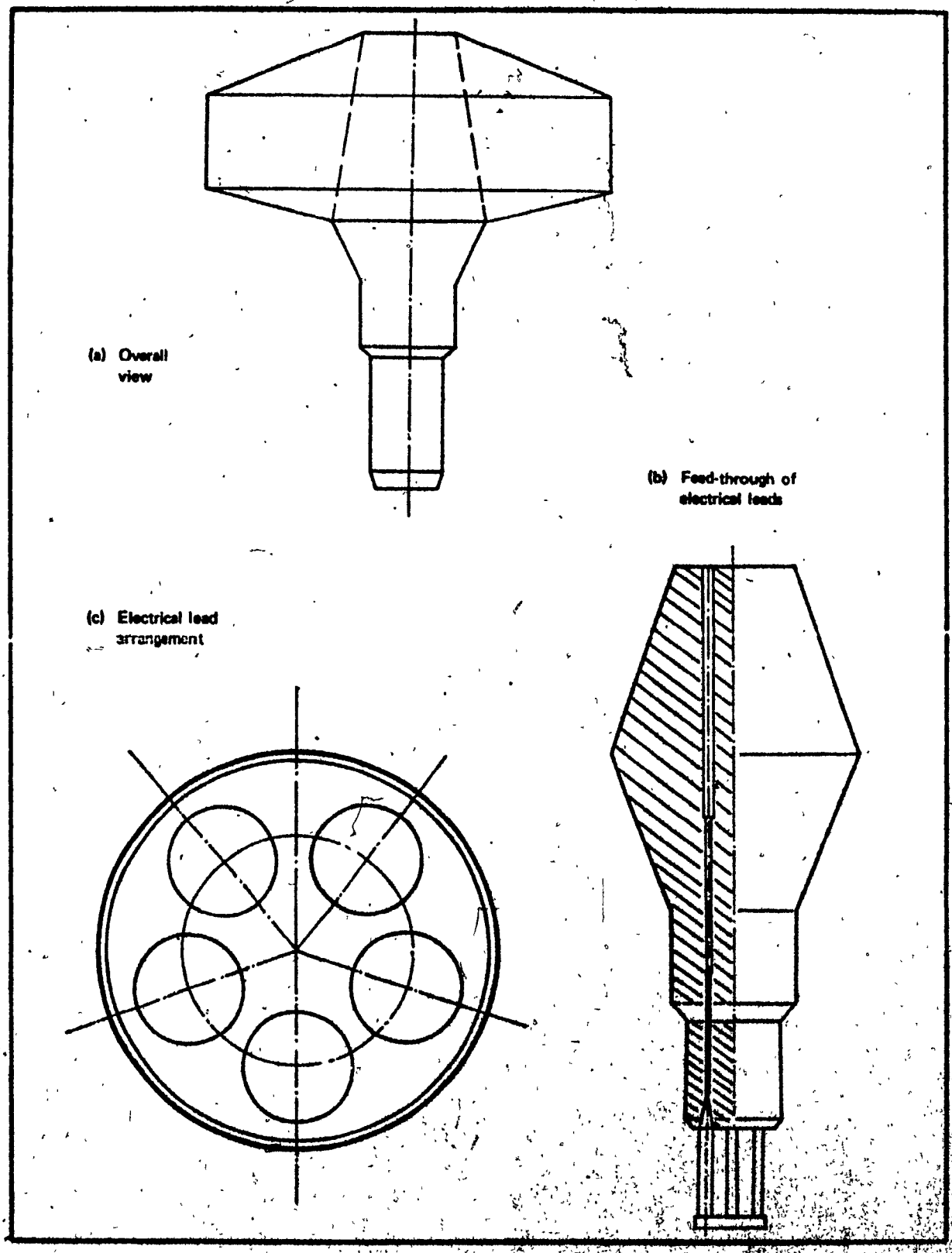

Fig. 3-6 Sample holder

3.3 Calculation of the Transition Pressure

The calculation of the theoretical transition pressures is based on the equations developed in Part I, subsection 2.3. With the aid of a developed computer program (see Appendix B) written in BASIC computer time sharing language, the lattice energies and the molecular volumes were calculated with a five digit accuracy. As a matter of interest, the "zone of indifference" of rubidium - chloride (RbCl) was investigated, theoretically, by calculating the energies, as a function of pressure. The computational tool used is essentially the same program as the above mentioned, re-written in FORTRAN time-sharing computer language. Here, double precision is used for the entering parameters with a 14-digit accuracy in the printed results.

4. RESULTS

4.1 Kinetic Aspect Data

The compilation of observed and calculated data follows. All related measurements were made at room temperature. The pressure was kept constant at each step for as long as a change in the resistance of the sample could be recorded. Then the pressure would be increased, kept constant, and the measurement repeated.

As a typical example, Figs. 4-1 and 4-2 indicate the variation of the logarithm of the resistance of $HgSe_{0.8}Te_{0.2}$ and $HgSe_{0.6}Te_{0.4}$ respectively, as a function of time. Taking the slope of these curves then, one obtains the logarithm of the rate of the resistance change as a function of pressure, as shown in Fig. 4-3. As it can be seen from these graphs, there is a linear dependence between the measured variables. This suggests a first order type kinetics for the alloys under study.

Furthermore, the "volume of activation" is calculated for the same alloys, utilizing the equation derived by Polanyi (14)

$$\left(\frac{\partial \ln k}{\partial P}\right)_T = \frac{\Delta V}{RT}$$

Substituting for $k = \frac{\Delta R}{\Delta t}$ and for $R = 1.987$ cal deg^{-1} mole^{-1} and $T = 300$ °K the above equation can be written as:

$$V^* = 24{,}200 \frac{\partial \ln\left(\frac{\Delta R}{\Delta t}\right)}{\partial P} \qquad (23)$$

Equation (23) is used in the calculations. The results are summarized in table I.

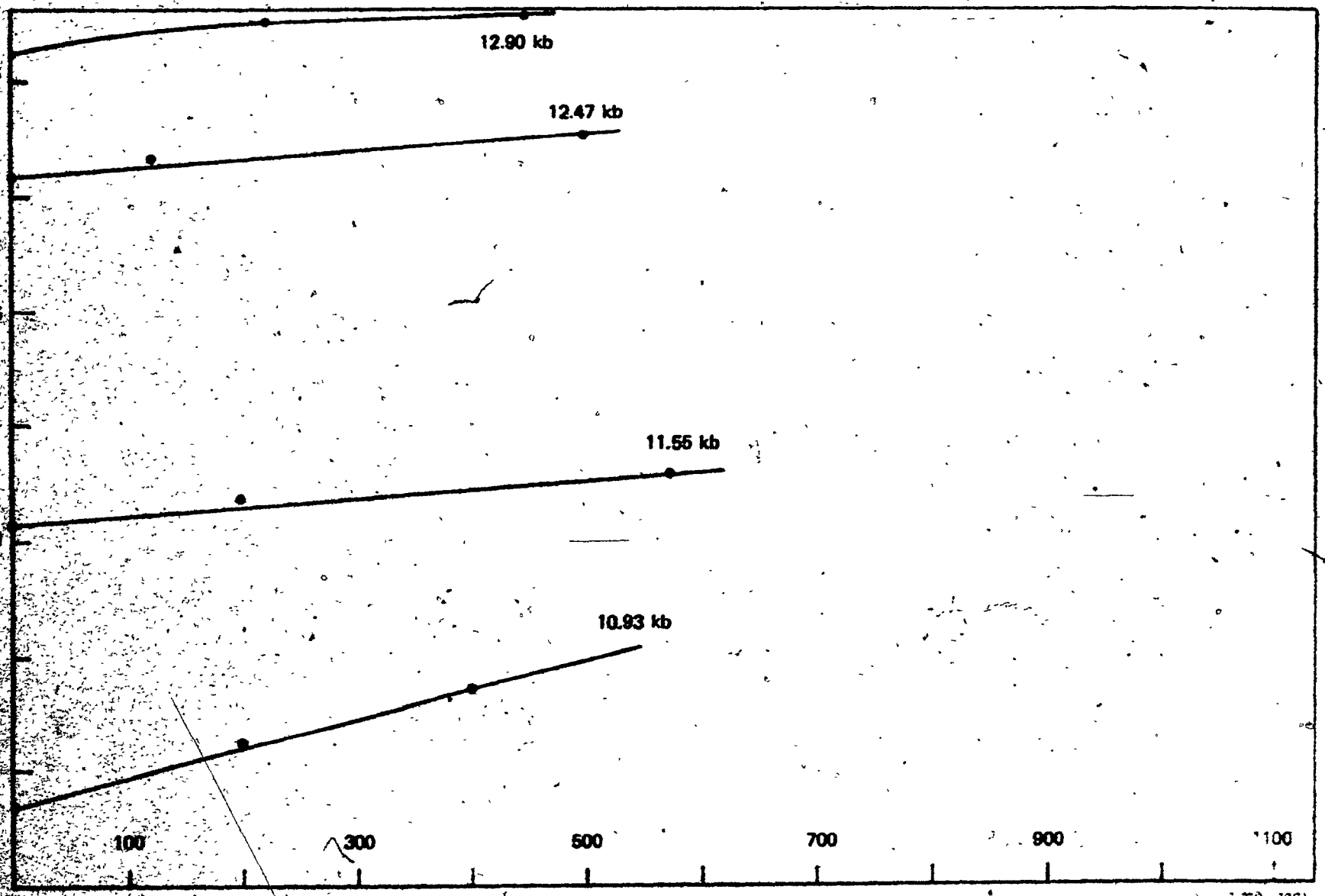

Fig. 4-1 Resistance variation of $HgSe_{0.8}$ $Te_{0.2}$ as a function of time

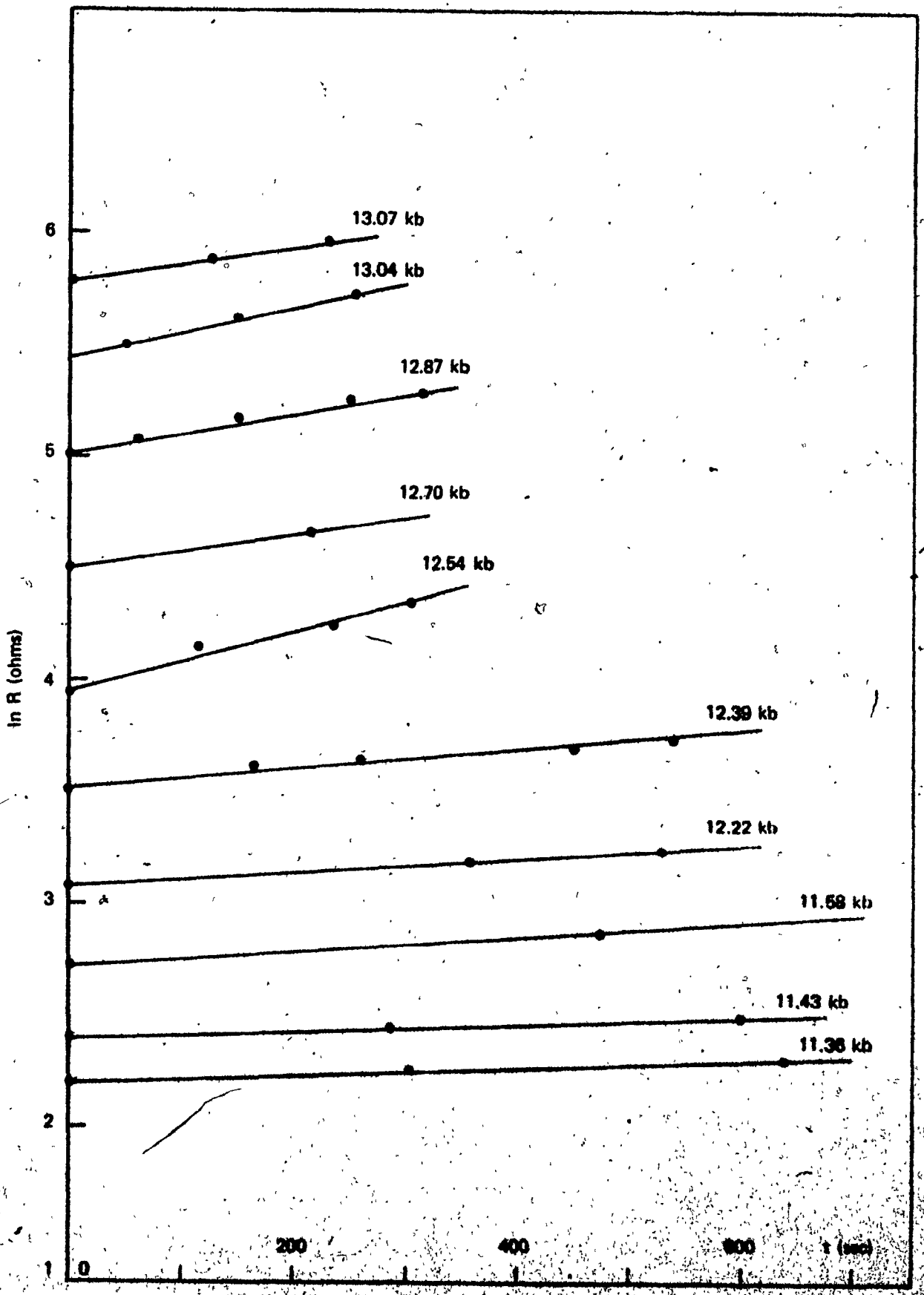

Fig. 4-2 Resistance Variation of Hg $\beta_{0.8}$ $T_{c_{0.8}}$ as a function of time

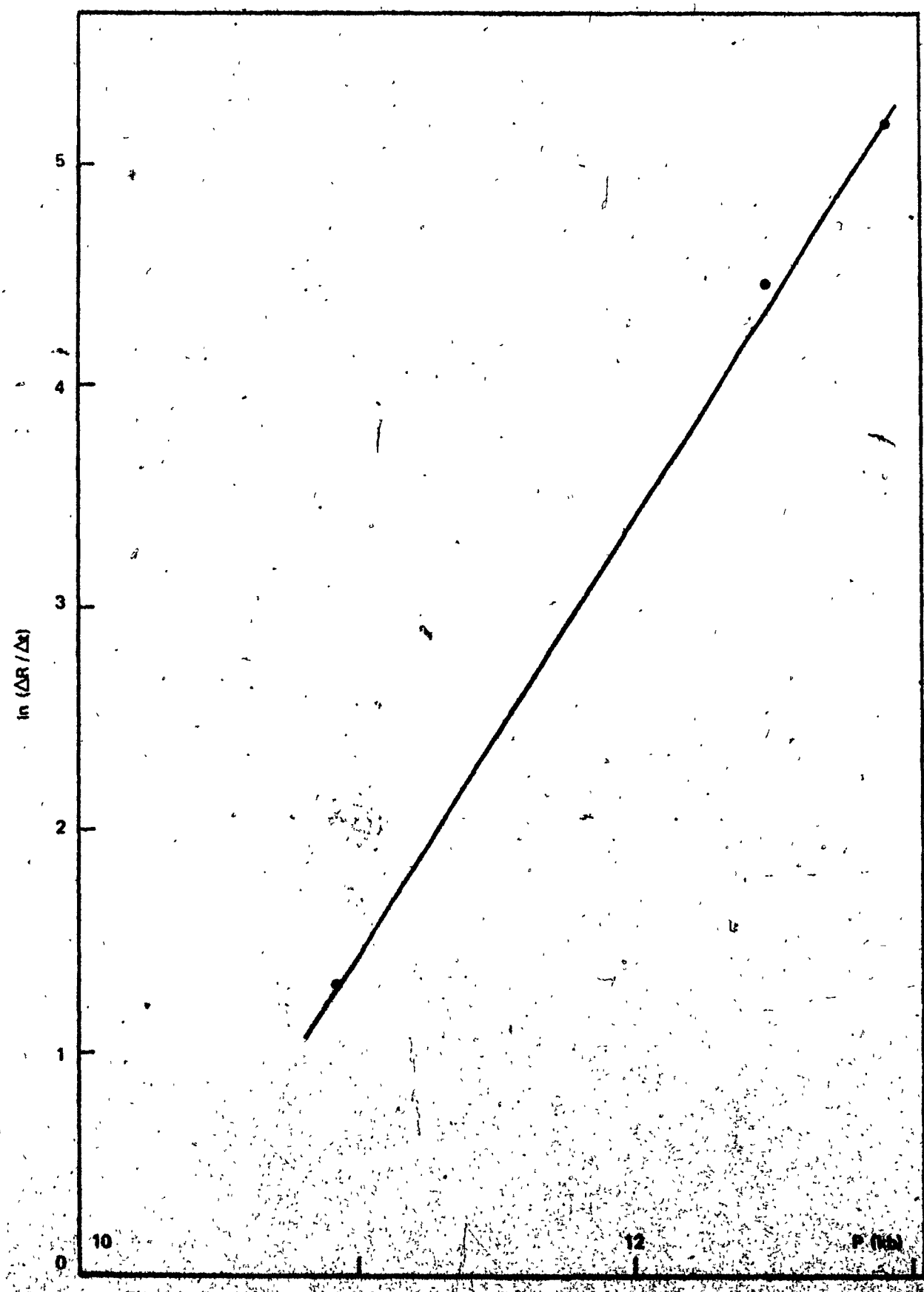

Fig. 4-3 Resistance rate variation of $Hg_{0.8}Tl_{0.2}$ as a function of pressure

TABLE I

VOLUME OF ACTIVATION OF $HgSe_xTe_{(1-x)}$ ALLOYS

ALLOY	VOLUME OF ACTIVATION V^* (cc $mole^{-1}$)
$HgSe_{0.8}Te_{0.2}$	47.6
$HgSe_{0.6}Te_{0.4}$	103
$HgSe_{0.4}Te_{0.6}$	387
$HgSe_{0.2}Te_{0.8}$	107.5

4.2 Calculated Transitions Pressures (Alkali Halides)

As it is mentioned in the previous section, these calculations were carried out using a computer program. In order to test its correctness along with its accuracy, a reproduction of the results obtained by Jacobs (11) for the alkali halides was attempted.

The flow chart together with the program listing (in BASIC computer time-sharing language) are shown in the Appendix B, Fig. B-1 and B-2 respectively. Table IX is a typical printout of the calculated lattice energies, volumes and the corresponding theoretical transition pressure, for the low and high pressure phases as a function of the nearest neighbour distance. The values shown correspond to those for the rubidium-chloride (RbCl). Table X is a typical printout of the coulomb and repulsive energy values at the transition pressure (middle row). Similar calculations were performed for rubidium-iodide (RbI), rubidium-bromide (RbBr), Potassium-chloride (KCl), Potassium-iodide (KI) and Potassium-Bromide (KBr). The results are in excellent agreement with those obtained by Jacobs, as it can be seen in tables II and III. Figs. 4-4 and 4-5 show the transition pressure variation as a function of the nearest neighbour distance. The linear dependence of the theoretically calculated transition pressure of RbCl as a function of the nearest neighbour distance is shown in Fig. 4-6.

The flowchart in Appendix B, Fig. B-3, shows the necessary modification required on the previously mentioned

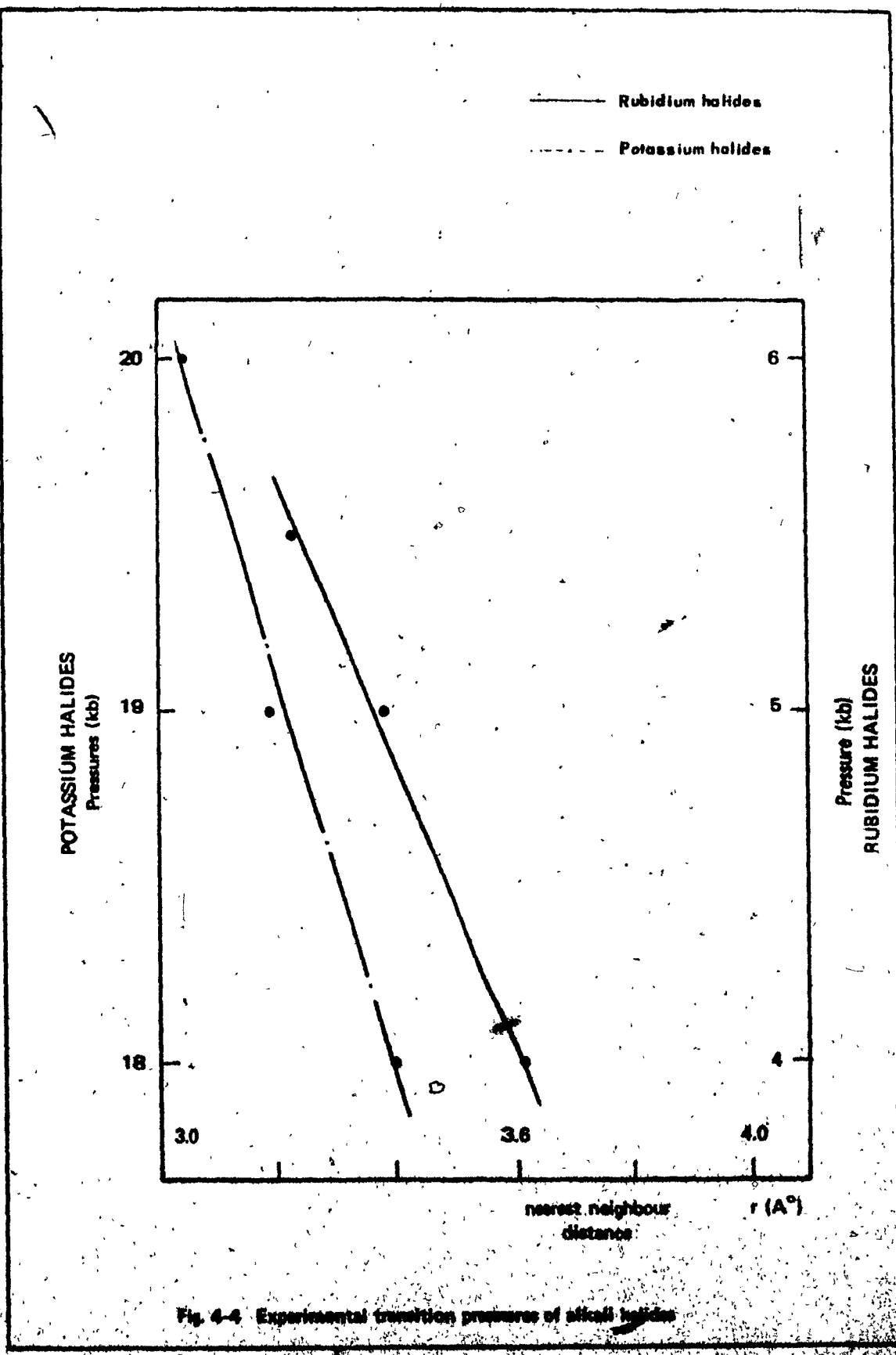

Fig. 4-4 Experimental transition pressures of alkali halides

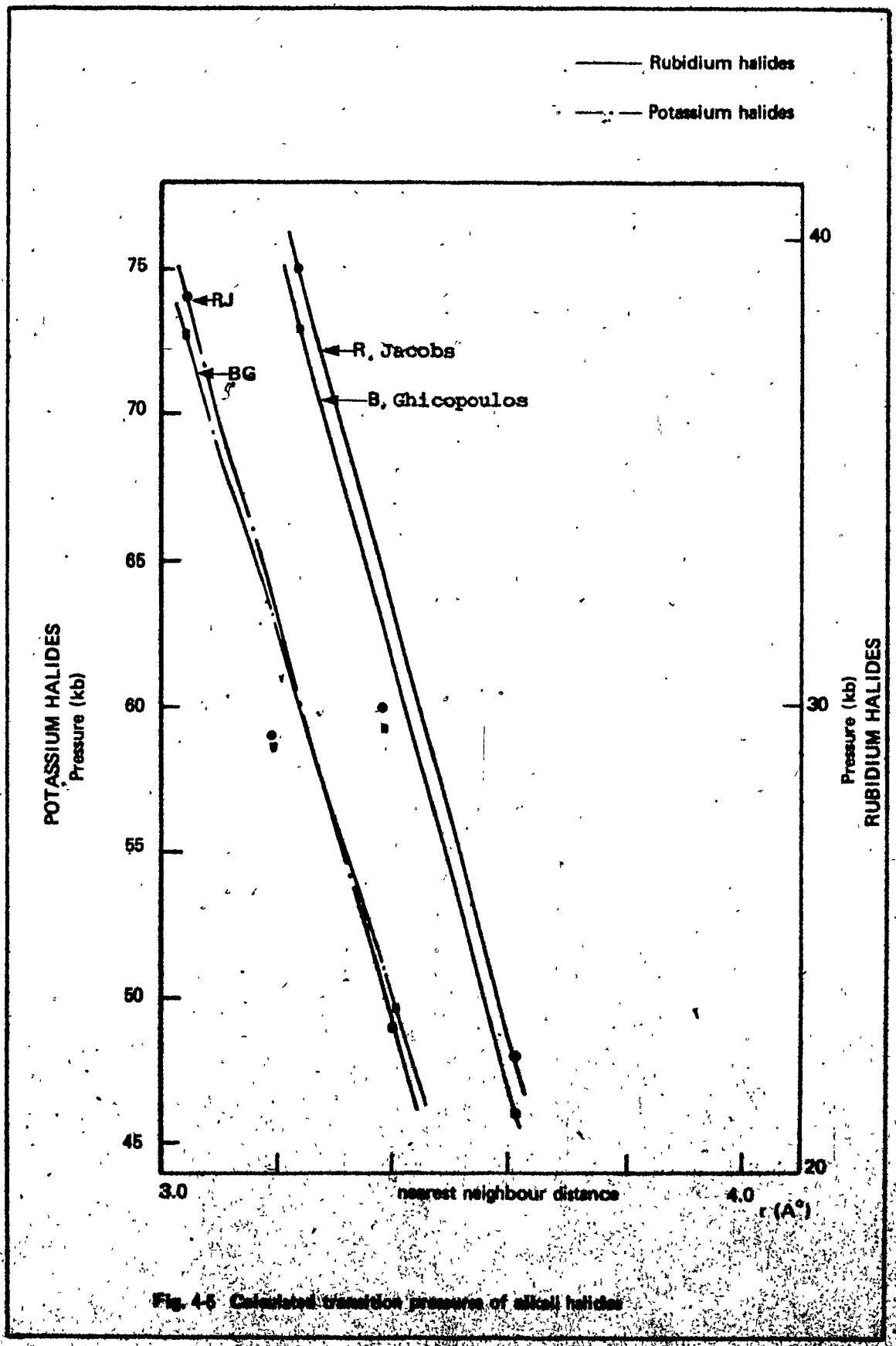

Fig. 4-5 Calculated transition pressures of alkali halides

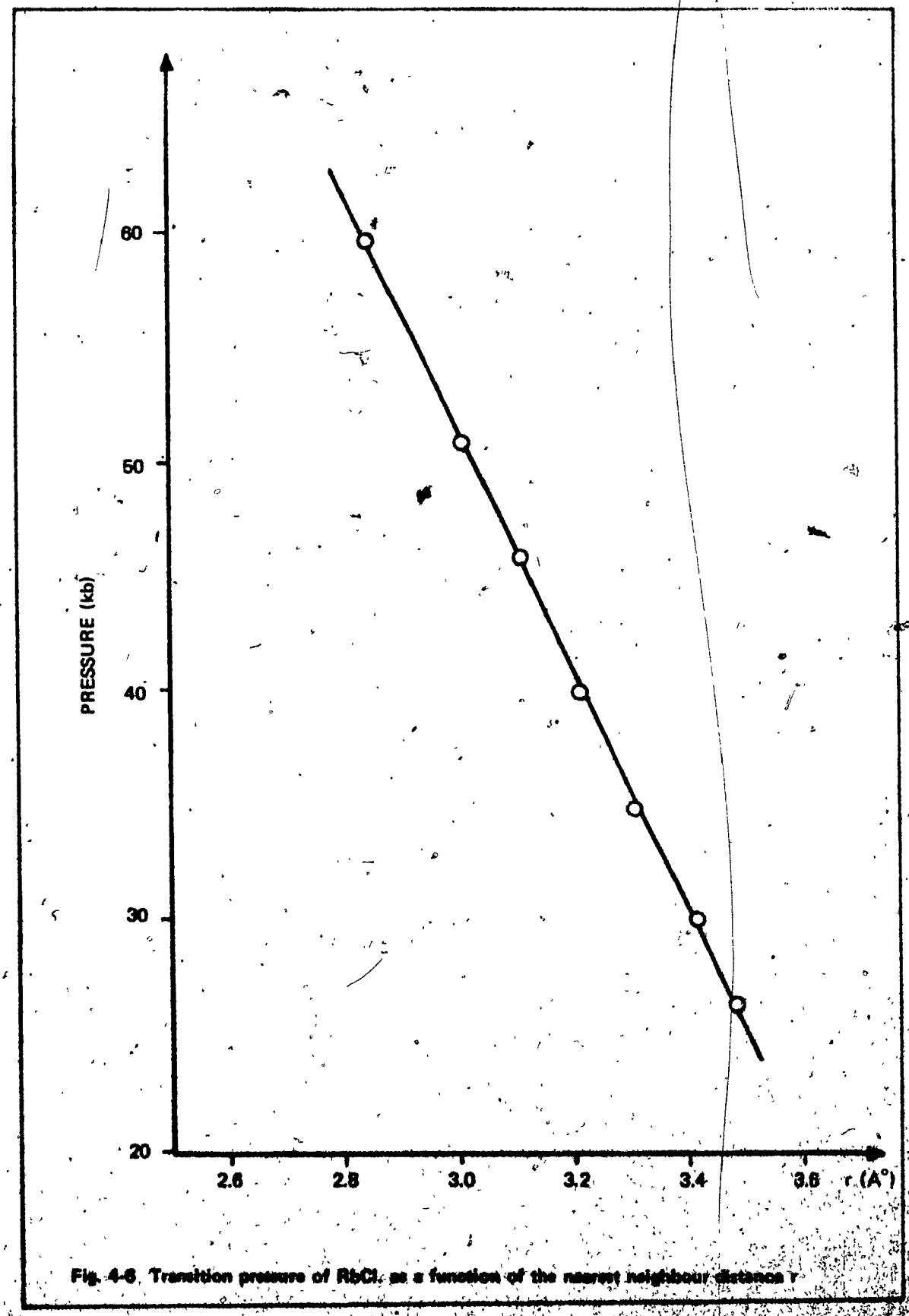

Fig. 4-6 Transition pressure of RbCl as a function of the nearest neighbour distance r

main program in order to examine the "zone of indifference". The listing of the program, written in FORTRAN, is as shown in Fig. B-4 whereas Table XI is a typical printout of the pressure and energy values at the low and high pressure phases. Plotting these values, with a 6-digit accuracy, one observes in Fig. 4-7 that, the two phases cross at one point only.

TABLE II

CALCULATED TRANSITION PARAMETERS IN RUBIDIUM HALIDES

PARAMETER	RbCl				RbBr				RbI			
	Low Press. Phase (f.c.)		High Press. Phase (b.c.)		Low Press. Phase (f.c.)		High Press. Phase (b.c.)		Low Press. Phase (f.c.)		High Press. Phase (b.c.)	
	RJ	BG	RJ	BG	RJ	BG	RJ	BG	RJ	BG	RJ	BG
r (10^{-8} cm)	3.24	3.24	3.39	3.39	3.38	3.38	3.54	3.54	3.61	3.61	3.78	3.78
E (10^{-12} ergs)	11.23	11.36	10.92	11.06	10.80	10.93	10.54	10.67	10.25	10.36	10.41	10.13
V (10^{-24} cm^3)	68.0	68.02	60.0	59.98	77.2	77.22	68.3	68.29	94.1	94.09	83.2	83.15
ΔV (10^{-24} cm^3)			8.0	8.04			8.9	8.93			10.9	10.94
P (kg/cm^2)			39,000	38,10-			30,000	29,703			22,000	21,681

TABLE III

CALCULATED TRANSITION PARAMETERS IN POTASSIUM HALIDES

PARAMETER	KCl				KBr				KI			
	Low Press. Phase (f.c.)		High Press. Phase (b.c.)		Low Press. Phase (f.c.)		High Press. Phase (b.c.)		Low Press. Phase (f.c.)		High Press. Phase (b.c.)	
	RJ	BG	RJ	BG	RJ	BG	RJ	BG	RJ	BG	RJ	BG
r (10^{-8} cm)	3.04	3.04	3.21	3.21	3.19	3.19	3.37	3.37	3.40	3.40	3.60	3.60
E (10^{-12} ergs)	11.61	11.75	11.24	11.38	11.14	11.27	10.80	10.93	10.51	10.64	10.19	10.31
V (10^{-24} cm^3)	56.2	56.18	51.0	50.92	64.9	64.92	59.0	58.92	78.6	78.60	71.9	71.83
ΔV (10^{-24} cm^3)			-5.2	5.26			5.9	6.00			6.7	6.77
P (Kg/cm^2)			74,000	72,858			59,000	58,688			49,000	49,883

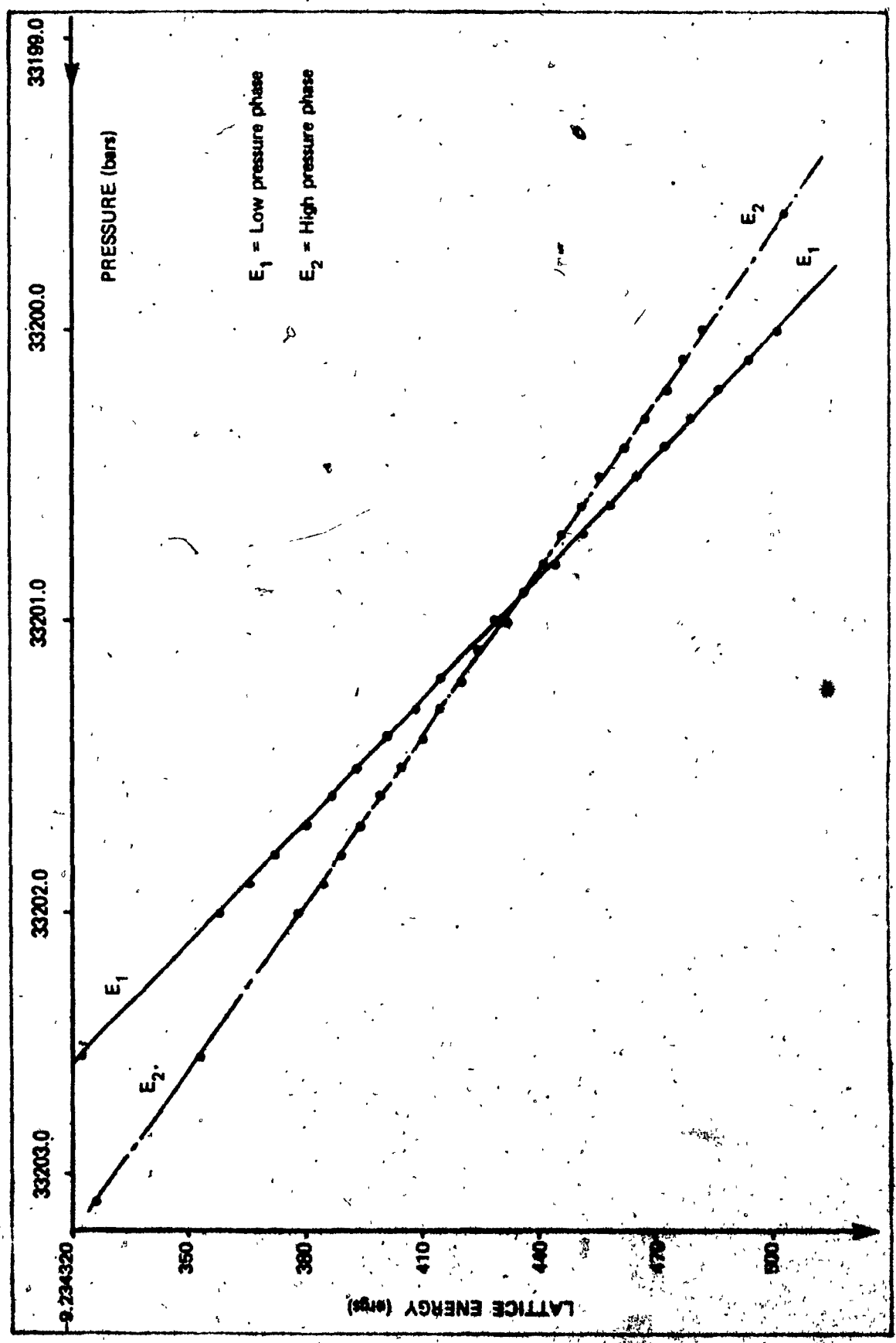

Fig. 4-7 Lattice energy of RbCl as a function of pressure

4.3 Calculated Transition Pressures - Mercury Chalcogenides

Having verified that the developed mathematical tool is reliable, it was further used to calculate the theoretical pressures of $HgSe_xTe_{(1-x)}$ compounds and their alloys. Some modifications were necessary to account for the difference in the nature of mercury chalcogenides as compared to alkali halides. The actual program, then, used is shown in the listing of Fig. C-1. The calculated pressures, along with the energy, molecular volumes and their differenoe for each phase are shown in Tables IV - VI . These values are calculated as a function of the nearest neighbour distance r for each of the compounds and their alloys, assumed to behave in a linear manner. This linear relationship is proven, as it can be seen in the printouts.

Furthermore and, for discussion purposes, the Coulomb and repulsive energy values are as indicated in Tables XV - XVII for each of the $HgSe_xTe_{(1-x)}$ compounds and their alloys. These results are summarized in the Tables IV, V and VI. The significance of some of the parameters shown therein will be discussed in the next section.

Fig. 4-8 depicts the theoretically calculated pressure as a function of the nearest neighbour distance r. The observed pressures, as determined by B. Lombos et al (12), and as shown in fig. 4-9, seem to be a linear function of composition. The agreement with the present results seems to be good.

TABLE IV

CALCULATED TRANSITION PARAMETERS IN MERCURY CHALCOGENIDES

PARAMETER	HgSe		$HgSe_{0.8}Te_{0.2}$		$HgSe_{0.6}Te_{0.4}$		$HgSe_{0.4}Te_{0.6}$		$HgSe_{0.8}Te_{0.2}$		HgTe	
	B3	B9	B3	B9	B3	B9	B3	B9	B3	B9	B3	B9
r (10^{-8} cm)	2.63	2.43	2.664	2.424	2.698	2.384	2.732	2.412	2.766	2.426	2.80	2.44
E (10^{-12} ergs)	11.28	11.26	11.08	11.06	10.82	10.79	10.52	10.47	10.19	10.12	9.84	9.74
V (10^{-24} cm^3)	55.93	53.81	58.13	55.73	60.39	57.26	62.70	58.43	65.07	59.81	67.50	61.01
ΔV (10^{-24} cm^3)		2.12		2.40		3.13		4.27		5.26		6.49
P (Kg/cm^2)		8,964		10,721		11,490		12,226		13,821		15,186

B3 = Sphalerite; B9 = Hexagonal Cinnabar

TABLE V

PROPORTIONAL VALUES OF VARIOUS PARAMETERS ENTERING THE THEORETICAL CALCULATION OF TRANSITION PRESSURES IN Hg CHALCOGENIDES

$HgSe_xTe_{(1-x)}$	ρ exp (10^{-8}cm)	$r^+ + r^-$ (10^{-8}cm)	δ (10^{-8}cm)	P (kb)	Ionicity (%)	r (10^{-8}cm)	Linear Δr (%)	$\Delta(c/a)$ (%)
HgSe	0.596	2.464	0.320	8.96	6	2.63	0	0.642
$HgSe_{0.8}Te_{0.2}$	0.566	2.523	0.289	10.72	5	2.664	20	0.632
$HgSe_{0.6}Te_{0.4}$	0.5476	2.585	0.257	11.49	4	2.698	40	0.622
$HgSe_{0.4}Te_{0.6}$	0.5386	2.647	0.225	12.22	3	2.732	60	0.612
$HgSe_{0.2}Te_{0.8}$	0.539	2.709	0.193	13.82	2	2.766	80	0.602
HgTe	0.54	2.773	0.159	15.18	1	2.80	100	0.590

TABLE VI

DIFFERENCE BETWEEN CALCULATED AND ADJUSTED EMPIRICAL CONSTANTS

Linear $\Delta\rho$ (%)	$\rho_{(calc)}$ (10^{-8}cm)	$\rho_{(exp)}$ (10^{-8}cm)	$\Delta\rho$ (10^{-8}cm)	a' calc	a' exp	Δ a' (calc-exp)
0	0.596	0.596	0.0	1.560	1.56	0.000
20	0.584	0.566	0.018	1.554	1.55	0.004
40	0.573	0.547	0.026	1.548	1.54	0.008
60	0.562	0.538	0.024	1.542	1.54	0.002
80	0.551	0.539	0.012	1.536	1.53	0.006
100	0.540	0.540	0.0	1.530	1.53	0.000

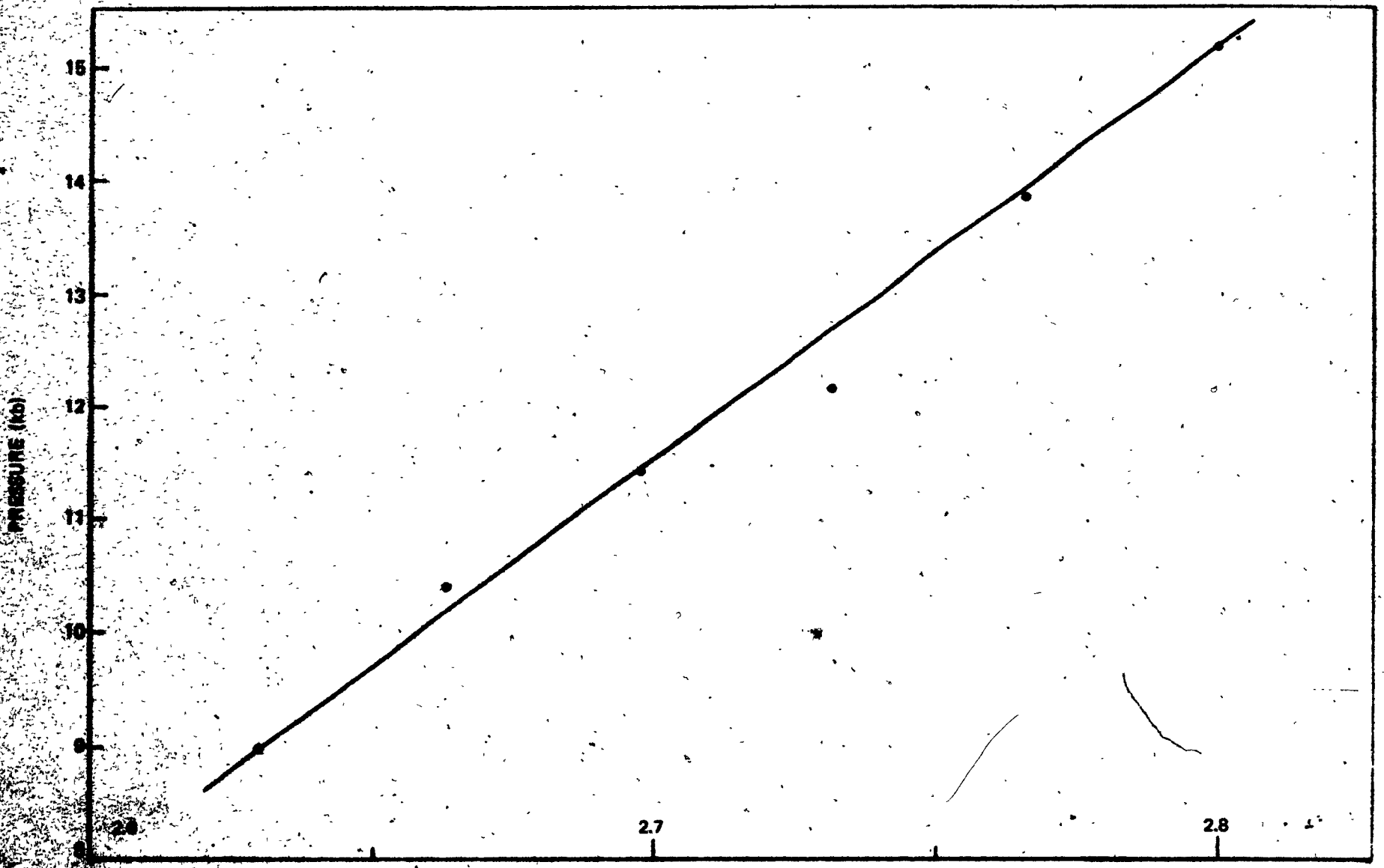

Fig. 4-8 Calculated transition pressures of $HgSe_x\ Te_{(1-x)}$ as a function of the nearest neighbour distance r

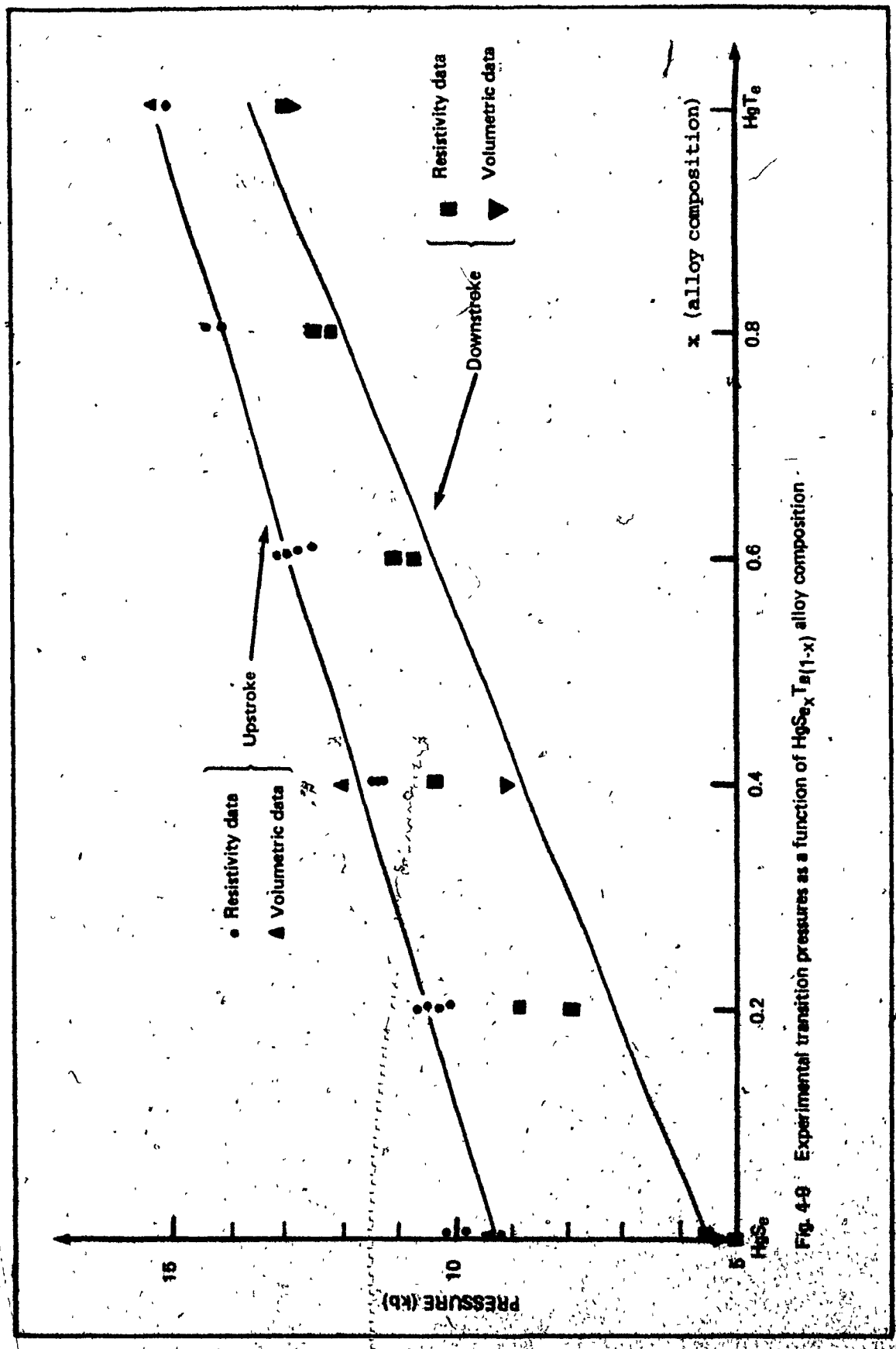

Fig. 4-9 Experimental transition pressures as a function of $HgSe_xTe_{(1-x)}$ alloy composition

5. DISCUSSION AND CONCLUSION

5.1 Discussion of Results

The data related to the resistance variation of the alloys under study, as a function of time, provide a means of determining the kinetics of the transitions occuring in each of the alloys separately. By assuming that, the transformed portion of the alloy into the high pressure phase, is proportional to its resistance variations, the relationship of the logarithm of the rate of change of the resistance as a function of pressure proved to be linear. From the kinetics point of view, this obeys the 1st order law and, therefore, it is concluded that the transitions are of the first order type. Other factors influencing the rate of the transition could be the change of the dimensions of the crystal under pressure, temperature, etc. so that when the two phases are in contact, a more accurate behaviour of the resistance of the material can be predicted. However, these parameters are quite difficult to measure on a continuous basis, i.e. during the transitions, and techniques need to be developed. A more complete understanding of the mechanism of the transition could then be achieved.

Furthermore, from the obtained data, the "volume of activation" is determined for each of the alloys. This quantity actually being a composite function, as suggested by Hamann (16), it could be of interest to attempt a comparison with the difference of the molecular volumes between the two phases, as obtained through the theoretical calculations of the transition pressures.

One observes that the trend, based on the numerical values obtained, is of the same direction, that is increasing.

In examining the zone of indifference, as shown in Fig. 4-7 one observes that for this particular case of RbCl, and at least from the theoretical point of view, there is no zone of indifference and the transition to the high pressure modification should proceed smoothly.

The dependence of the theoretically calculated pressures on the nearest neighbour distance, in the mercury chalcogenides, is of an opposite nature when compared with that of the alkali halides. Although both are linear, with respect to (1/r), the pressure is decreasing as the (1/r) decreases in case of the alkali halides, whereas in the mercury chalcogenides the pressure is increasing as the (1/r) decreases.

Having observed that the influence on the total energy and the magnitude of the van der Waals forces in the alkali halides was quite negligible, it was decided to omit these from the subsequent calculations on the $HgSe_xTe_{(1-x)}$. As it can be seen from the obtained results, the attractive force (coulomb term) is primarily dominating with the repulsive term decaying rapidly in an exponential manner (see equation 6).

In calculating the repulsive energy terms it was mentioned that, the constant ρ is experimentally adjusted. This implies that another existing variable should be selected as a reference so that the value of ρ can be adjusted towards it.

Thus, in the case of the halides, for example, the value of ρ is experimentally adjusted towards the calculated radii, r^+ and r^-. In our study, since the experimental values of the transition pressures are available, that is P = 9kb for HgSe, and P = 15 kb for HgTe, the value of the corresponding ρ is determined and the theoretical values are normalized to the two experimental ones (by adjusting the ρ through the iteration process). By taking into consideration the assumed linearity of the nearest neighbour distance and the ρ for the alloys, the respective values of ρ are shown in Table VI. Minor adjustment of ρ is necessary because the repulsive term is very sensitive to it, although it is smaller than the coulomb term, with the latter dominating. The (1/r) linear dependence then, of the transition pressure, is as expected, since it is a linear function of the alloy composition.

5.2 Conclusion

The kinetics of the pressure induced solid solid phase transitions of the mercury chalcogenides, $HgSe_xTe_{(1-x)}$ compounds and alloys, was investigated by the method of the resistance variation. It is determined to be of the 1st order type.

The volume of activation for the $HgSe_xTe_{(1-x)}$ compounds has been calculated with the results indicating an increasing trend, from the lower to the higher transition pressures of the same alloys.

A theoretical investigation of the "zone of indifference" was attempted, for the RbCl. The low and high pressure energy curves intersect at one point only suggesting no such zone existing.

Further developments in the existing high pressure techniques could facilitate more detailed and therefore more accurate study of the phenomena associated with the mechanisms of the polymorphic transformations.

The emphasis of the analysis being on the ionic character of bonding of $HgSe_xTe_{(1-x)}$ compounds and their alloys, the amount of ionicity is explicitly determined. This permits a more accurate computation of the lattice energies at the low and high pressure phases.

In analyzing the energy terms, it is concluded that, the Coulomb term, representing the attractive force, is of primary importance dominating over the repulsive energy term.

In addition, the detailed computation of the latter indicated that, it is extremely dependent on the value of the normalizing variable ρ.

Finally, in the present work, the theoretical transition pressures for these compounds and their alloys, were determined, being in good agreement with those experimentally found. It has also been shown that the dependence of the pressure induced phase transitions on the nearest neighbour distance, is linear.

REFERENCES

(1) P.W. Bridgman — "Change of phase under pressure I. The phase diagram of eleven substances with special reference to the melting curve". Phys. Rev. 3, 126-141, 153-203 (1914).

(2) P.W. Bridgman — "Change of phase under pressure II. New melting curves with a general thermodynamic discussion of melting". Phys. Rev. 6, 1-33, 94-115 (1915).

(3) P.W. Bridgman — "Polymorphic transformations of solids under pressure". Proc. Am. Acad. Sci. 51, 55-124 (1915).

(4) P.W. Bridgman — "The effect of pressure on polymorphic transtions of solids". Proc. Nat. Acad. Sci. U.S. 1, 513-516 (1915).

(5) P.W. Bridgman — "The velocity of polymorphic changes between solids". Proc. Am. Acad. Sci. 52, 57-88 (1916).

(6) A. Jayaraman et al. — "Melting and polymorphic transitions for some group II - VI compounds at high pressures". Phys. Rev. 130, 2277-2283 (1963).

(7) G. Kennedy and P. LaMori — "The pressures of some solid-solid transitions". J. of geophys research, 67, No. 2, 851-856 (1962).

(8) C. Pistorius — "Polymorphic transitions of the alkali bromides and iodides at high pressures". J. of Phys. Chem. Solids, 26, 1003-1011 (1965).

(9) B. Lombos et al. — "Pressure effect on the rate of phase transition in mercury Telluride". Phys. Earth Planet Interiors, 3, 511-512 (1970).

(10) B. Lombos et al. — "Kinetic aspect of polymorphic transitions induced by high pressures". Proc. 1st Intern., Conf. Calorimetry and Thermodyn., Warsaw (1969).

(11) R. Jacobs — "Polymorphic transitions in metallic halides". Phys. Rev. 54, 468 (1938).

(12) B. Lombos et al — "Pressure induced phase transitions in mercury chalcogenides". Chem. Phys. let. 18, No. 1, Jan. (1973).

(13) R. Bradley — "High pressure physics" v. 1, Acad. Press (1963).

(14) M. Evans and Polanyi — "Some applications of the transition state method to the calculation of reaction velocities, especially in solution". Trans. Faraday Soc. 31, 875 (1935).

(15) A. Onodera — "Kinetics of the polymorphic transitions of cadmium chalcogenides under high pressure". The Review of Phys. Chem. of Japan 41, No. 1 & 2 (1971).

(16) S.D. Hamann — "Chemical kinetics" in R.S. Bradley ed. High pressure physics and chemistry. Vol. 2, (1963).

(17) M. Huggins and J. Mayer — "Interatomic distances in crystals of the alkali halides". J. of Chem. Phys. 1, 643 (1933).

(18) J. Mayer — "Dispersion and polarisability and the van der Waals potential in the alkali halides". J. of Chem. Phys. 1, 270 (1933).

(19) L. Pauling — "The sizes of ions and their influence on the properties of salt-like compounds" Zeit f. Krist 67, 377 (1928).

(20) A. Mariano and E. Warekois — "High pressure phases of some compounds of group II - VI". Sci. 142, 672 (1963).

(21) L. Pauling — "The nature of the chemical bond". Cornell Univ. Press (1960).

(22) K. Aurivillius — "On the crystal structure of cinnabar". Acta. Chem. Scand. 4, 1413-1436 (1950).

APPENDICES

APPENDIX A

CALCULATIONS

In order to calculate the theoretical pressure, as given by equation (18), the volumes at the low pressure and high pressure modification must be determined.

1. Unit Cell Volume Alkali Halides

At the low pressure modification, the lattice is of the sodium chloride (NaCl) type, Fig. 2-2(a) and the volume of the unit cell will be given by:

$V_1 = a^3$ with $a = 2r$ and r = nearest neighbour distance

Since there are 4 Na atoms and 4 Cl atoms in the unit cell, the volume per Na or Cl atom will be:

$$V_1 = \frac{a^3}{4} = 2r^3 \tag{24}$$

At the high pressure modification, the lattice is of the cesium chloride (CsCl) type, Fig. 2-2(b) and the volume of the unit cell will be given by:

$$V_2 = a^3 \quad \text{with} \quad a = \frac{2r}{\sqrt{3}} \tag{25}$$

Since there is 1 Cl atom and 1 Cs atom in the unit cell, the volume per Cs or Cl atom will be:

$$V_2 = a^3 = \frac{8r^3}{(\sqrt{3})^3} \tag{26}$$

2. c'_{ij} Factor - Mercury Chalcogenides

The determination of the c'_{ij} factor as per equations (10) and (11) is as follows:

We have that

Hg: closed shell $(5s^2 5p^6 5d^{10})6s^2$

Se: $1s^2)2s^2 2p^6)3s^2 3p^6 3d^{10})4s^2 4p^4$

Te: $1s^2)2s^2 2p^6)3s^2 3p^6 3d^{10})4s^2 4p^6 4d^{10})5s^2 5p^4$

and the valence shells are as follows:

HgSe: $4s^2 4p^6$ HgTe: $5s^2 5p^6$

then,

$$c'_{+} = \frac{c'_{++}}{c'_{\pm}} = \frac{1 + 2/18 + 2/18}{1 + 2/18 - 2/8} = \frac{1 + 2/9}{1 + 1/9 - \frac{1}{4}} = \frac{1.222}{0.861} = 1.42$$

$$c'_{-} = \frac{c'_{--}}{c'_{\pm}} = \frac{1 - 2/8 - 2/8}{0.861} = \frac{1 - 0.5}{0.861} = 0.58$$

The required c'_{ij} factors then will be of the same numerical value for both HgSe and HgTe since the outer shells s and p have the same number of electrons, as indicated above.

Thus,

$$c'_{++} = 1.222 \quad c'_{+-} = 0.861 \quad c'_{--} = 0.5$$

3. Unit Cell Volumes - Mercury Chalcogenides

The calculation of the volumes at the two phases is as follows:

At the low pressure modification, the lattice is of the sphalerite (ZnS) structure type, Fig. 2-3 (a). Its parameters, for HgSe and HgTe have been determined by Mariano and Warekois (20) using X-ray technique. They are as shown in Table VII. The volume of the unit cell will be given by:

$$V_1 = a^3 \quad \text{with} \quad a = \frac{4r}{\sqrt{3}} \tag{27}$$

Since there are 4 atoms in the unit cell, the volume per atom will be:

$$V_1 = \frac{a^3}{4} = \frac{64r^3}{4\sqrt{2}} = \frac{64r^3}{5.2} = (3.075)\, r^3 \tag{28}$$

At the high pressure modification, the lattice is of the hexagonal cinnabar (HgS) structure type, Fig. 2-3 (b). The volume of the unit cell will be given by:

$$V_2 = \frac{a^2\sqrt{3}c}{2} \tag{29}$$

Where a,c the lattice parameters shown in table VII.

Since there are 3 atoms in the unit cell, the volume/atom then will be given by:

$$V_2 = \frac{a^2 c\sqrt{3}}{6} \tag{30}$$

By taking into consideration the coordination of the atoms in the unit cell, the distances between like and unlike or, nearest, neighbours can be easily be determined. Refer to Fig. A-1.

The atoms within the unit cell, as shown in Fig. A-2, form a spiral chain.

The necessary data are summarized in table VII.

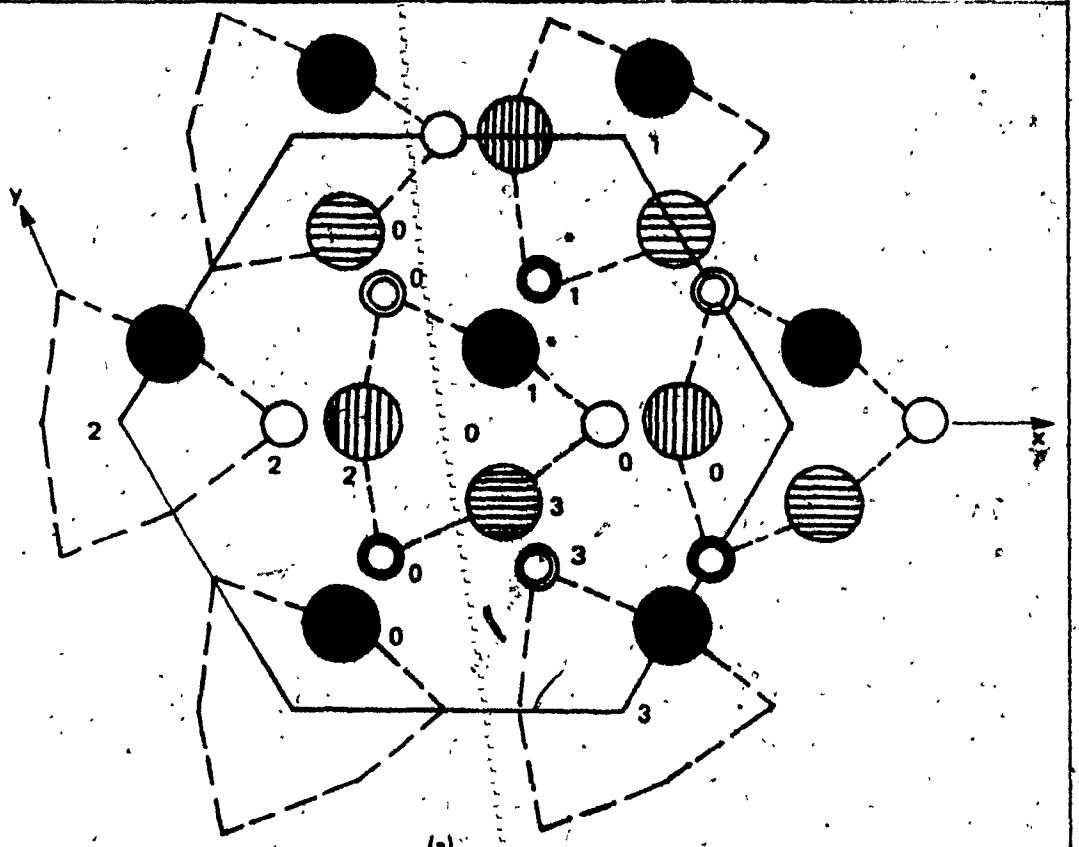

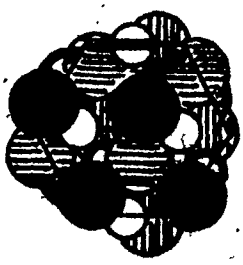

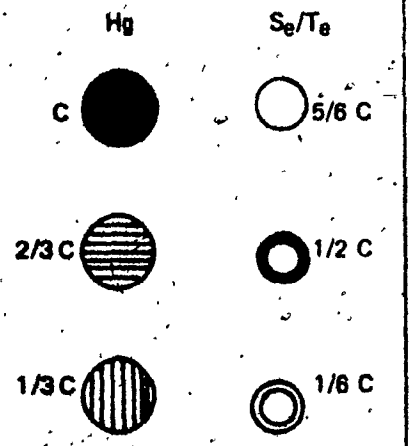

Fig. A-1 Cinnaber lattice structure (a) x,y projection (b) Contents of three unit cells

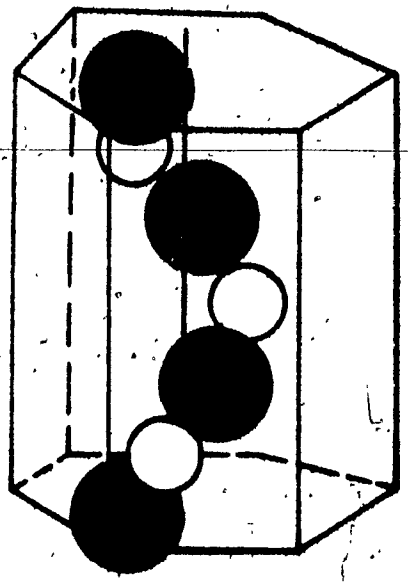

(a)

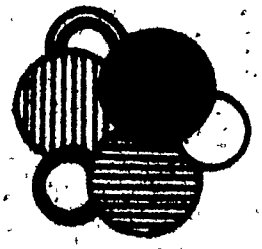

(b)

Fig. A-2 Cinnabar unit cell (a) Spiral chain, (b) xy projection of chain

TABLE VII

LATTICE PARAMETERS OF THE SPHALERITE AND CINNABAR STRUCTURES

CRYSTAL STRUCTURE	PARAMETER (A^o)	LOW PRESSURE MODIFICATION		HIGH PRESSURE MODIFICATION	
		HgSe	HgTe	HgSe	HgTe
SPHALERITE	a	6.09	6.44		
	Nearest Neighbour Distance	2.63	2.80		
	Like Neighbour Distance	$a/\sqrt{2}$	$a/\sqrt{2}$		
CINNABAR	a			4.32	4.46
	c			9.68	9.17
	Nearest Neighbour Distance			2.43	2.44
	Like Neighbour Distance			3.79	3.73

4. Ionic Character - Mercury Chalcogenides

The calculation of the ionic character of the bond, as suggested by L. Pauling (21), is given by the equation:

$$I = 1 - e^{-\frac{1}{4}(x_i - x_j)} \quad (\%) \qquad (19)$$

where:

x_i = electronegativity of Hg^+

x_j = electronegativity of Se^- or Te^-

The electronegativity values for the compounds HgSe and HgTe, can be calculated by taking into consideration the electronegativities of their elements. The latter have been calculated by L. Pauling (21). The difference, then, in electronegativity as required by equation (19) will determine the amount of the partial ionic character of the bonds. The assumed amount of ionic character of the bonds in their alloys, is taken to be proportional to the two compound values. The results are summarized in the Table VIII.

TABLE VIII

ELECTRONEGATIVITY AND AMOUNT OF IONIC CHARACTER VALUES OF Hg, Se, Te

ELEMENT	ELECTRO-NEGATIVITY	ELECTRONEGATIVITY DIFFERENCE		AMOUNT OF IONIC CHARACTER	
		HgSe	HgTe	HgSe	HgTe
Hg	1.9	0.5		6%	
Se	2.4		0.2		1%
Te	2.1				

APPENDIX B

COMPUTERIZED PROCEDURE - RbCl

Description

The calculation of the equations involved in determining the theoretical transition pressure P, was performed on a digital computer.

The main program, as is shown in Fig. B-2, is written in the time-sharing BASIC computer language. This allows for maximum flexibility when in the conversational mode.

This main program was used to reproduce the results obtained by R. Jacobs (11) for the case of the alkali halides. In addition, for the investigation of the "zone of indifference" (on a theoretical basis) minor modifications of this program were required. The modified program is as shown in Fig. B-4. This modified program is written in time-sharing FORTRAN computer language, since an extended digital value, for the lattice energies, was required. The results are as shown in Table XI. The flow charts for these two programs are shown in Fig. B-1 and B-3.

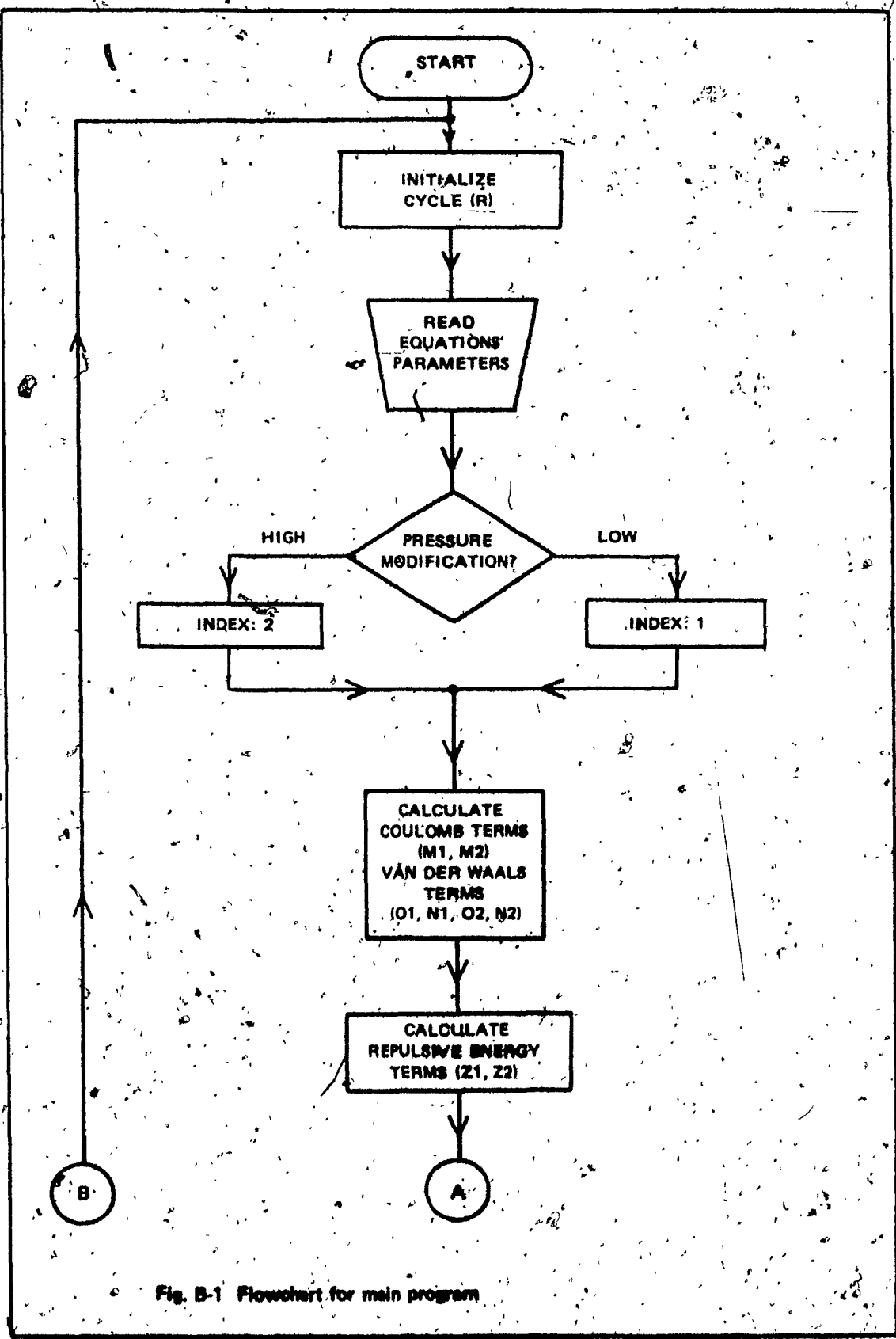

Fig. B-1 Flowchart for main program

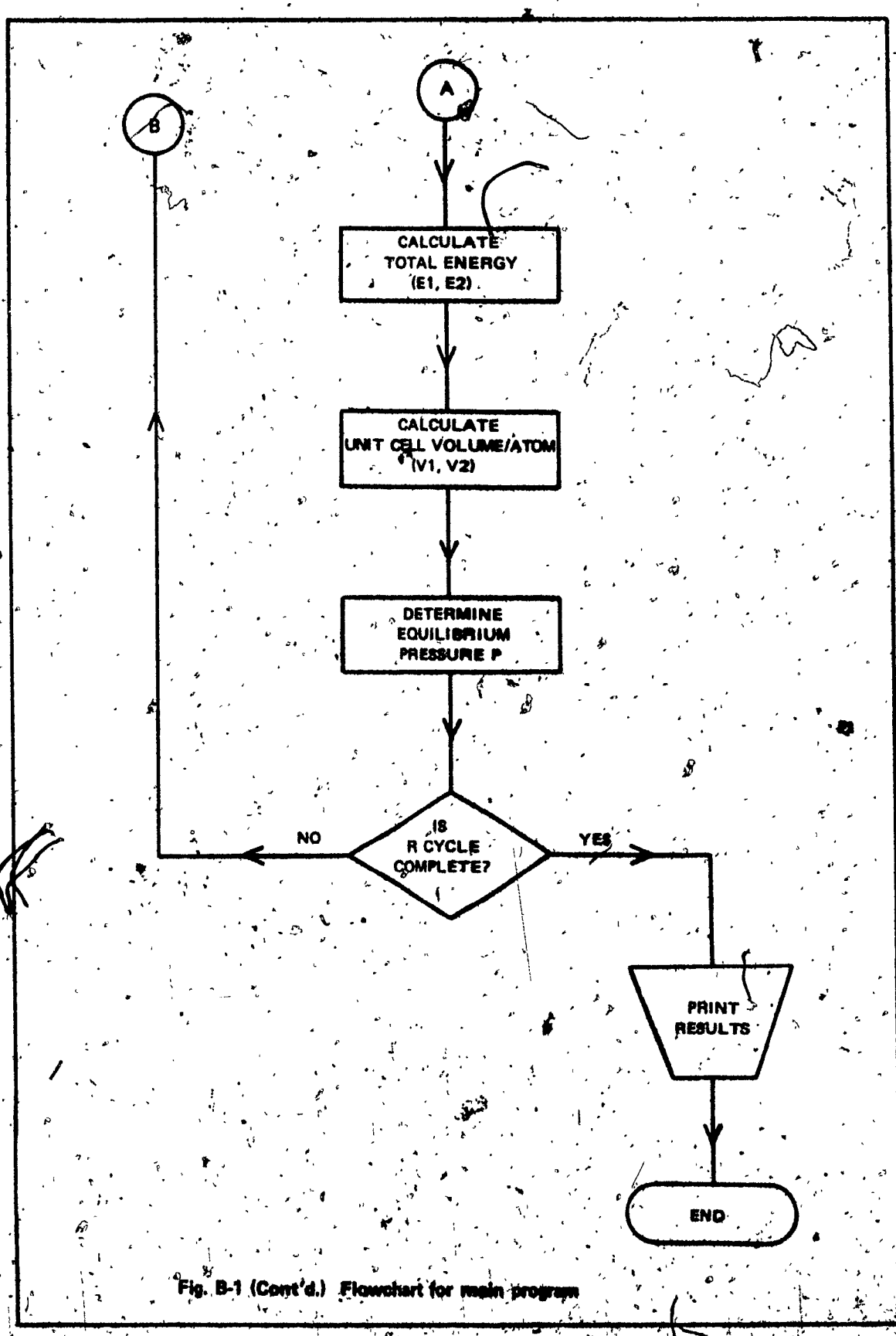

Fig. B-1 (Cont'd.) Flowchart for main program

```
5    MARGIN=0,132
10 FOR R=3.22 TO 3.26 STEP 0.01
15    READ A,A1,E,C,D,B,C1,M,X,Z,Y,C2,M3,C3,D1,C4,D2,M4,M5,A2,A3
20    LET W1=((A*(E^2))/R)*1E8
25    LET O1=C/(R^6)
30    LET N1=D/(R^8)
35    LET I1=W1+N1+O1
40    LET R1=R*1E-8
45    LET Y1=B*C1*M*(EXP(((X+Z)-R1)/Y))
50    LET S1=(C2/C1)*(M3/(2*M))*A1*(1+(C3/C2)*(EXP((-2*D1)/Y)))*(EXP(D1/Y))
55    LET Y2=Y1*((S1/A1)*(EXP(-((A1-1)*R1)/Y)))
60    LET Z1=Y1+Y2
65    LET E1=-I1+Z1
70    LET V1=2*(R1^3)
75    LET R2=R+0.15
80    LET W2=((A3*(E^2))/R2)*1E8
85    LET O2=C4/(R2^6)
90    LET N2=D2/(R2^8)
95    LET I2=W2+O2+N2
100   LET R3=R2*1E-8
105   LET Y3=B*C1*M4*(EXP(((X+Z)-R3)/Y))
110  LET S2=(C2/C1)*(M5/(2*M4))*A2*(1+(C3/C2)*(EXP((-2*D1)/Y)))*(EXP(D1/Y))
115   LET Y4=Y3*((S2/A2)*(EXP(-((A2-1)*R3)/Y)))
120   LET Z2=Y3+Y4
125   LET E2=-I2+Z2
130   LET V2=(8*(R3^3))/(SQR(3)^3)
135  LET P=((E2-E1)/(V1-V2))*(1.019*1E-6)
140 PRINT R1;TAB(16);E1;TAB(32);V1;TAB(49);R3;TAB(65);E2;TAB(81);V2;TAB(97);P
145   RESTORE
150   NEXT R
155   DATA 1.7476,1.1,4.7956E-10,591E-12,960E-12,1E-12,1,6,1.320E-8
160   DATA 1.4756E-5,0.345E-8,0.75,12,1.25,0.155E-8,1023E-12,1470E-12,8,5,1.1547
165   DATA 1.7626
170   STOP
```

Fig. B-2 Main program

TABLE IX Calculation of the theoretical transition pressures of RbCl

r_1 (cm)	E_1 (ergs)	V_1 (cm^3)	r_2 (cm)	E_2 (ergs)	V_2 (cm^3)	P (kg/cm^2)
2.77000e-08	-9.19419e-12	4.25079e-23	2.92000e-08	-9.13623e-12	3.83115e-23	61004.54
2.78000e-08	-9.50040e-12	4.29592e-23	2.93000e-08	-9.24179e-12	3.87267e-23	61754
2.79000e-08	-9.61406e-12	4.34151e-23	2.94000e-08	-9.34620e-12	3.91245e-23	61400.06
2.80000e-08	-9.71034e-12	4.39140e-23	2.95000e-08	-9.44441e-12	3.95252e-23	63127.2
2.81000e-08	-9.81120e-12	4.43761e-23	2.96000e-08	-9.53924e-12	3.99245e-23	62754.42
2.82000e-08	-9.91615e-12	4.48515e-23	2.97000e-08	-9.62974e-12	4.03345e-23	62357.5
2.83000e-08	-9.99504e-12	4.53104e-23	2.98000e-08	-9.71638e-12	4.07431e-23	61927.03
2.84000e-08	-1.00511e-11	4.57725e-23	2.99000e-08	-9.79913e-12	4.11549e-23	61470.32
2.85000e-08	-1.01613e-11	4.62382e-23	3.00000e-08	-9.87830e-12	4.15693e-23	60949.61
2.86000e-08	-1.02349e-11	4.67073e-23	3.01000e-08	-9.95394e-12	4.19863e-23	60487.50
2.87000e-08	-1.03130e-11	4.72798e-23	3.02000e-08	-1.00262e-11	4.24061e-23	59960.49
2.88000e-08	-1.03835e-11	4.77757e-23	3.03000e-08	-1.00951e-11	4.28284e-23	59424.25
2.89000e-08	-1.04509e-11	4.82791e-23	3.04000e-08	-1.01607e-11	4.32542e-23	58875.2
2.90000e-08	-1.05149e-11	4.87739e-23	3.05000e-08	-1.02234e-11	4.36825e-23	58305.69
2.91000e-08	-1.05759e-11	4.92843e-23	3.06000e-08	-1.02830e-11	4.41135e-23	57730.62
2.92000e-08	-1.06339e-11	4.97742e-23	3.07000e-08	-1.03397e-11	4.45475e-23	57142.5
2.93000e-08	-1.06889e-11	5.03175e-23	3.08000e-08	-1.03935e-11	4.49842e-23	56545.45
2.94000e-08	-1.07412e-11	5.08243e-23	3.09000e-08	-1.04447e-11	4.54234e-23	55941.76
2.95000e-08	-1.07907e-11	5.13447e-23	3.10000e-08	-1.04932e-11	4.58662e-23	55331.54
2.96000e-08	-1.08375e-11	5.18585e-23	3.11000e-08	-1.05391e-11	4.63115e-23	54716.55
2.97000e-08	-1.08819e-11	5.23961e-23	3.12000e-08	-1.05826e-11	4.67597e-23	54094.04
2.98000e-08	-1.09237e-11	5.29272e-23	3.13000e-08	-1.06237e-11	4.72103e-23	53475.07
2.99000e-08	-1.09632e-11	5.34513e-23	3.14000e-08	-1.06625e-11	4.76647e-23	52851.62
3.00000e-08	-1.10003e-11	5.40000e-23	3.15000e-08	-1.06992e-11	4.81215e-23	52220.37
3.01000e-08	-1.10352e-11	5.45413e-23	3.16000e-08	-1.07334e-11	4.85813e-23	51630.54
3.02000e-08	-1.10680e-11	5.50872e-23	3.17000e-08	-1.07657e-11	4.90443e-23	50974.94
3.03000e-08	-1.10987e-11	5.56362e-23	3.18000e-08	-1.07959e-11	4.95095e-23	50350.02
3.04000e-08	-1.11273e-11	5.61899e-23	3.19000e-08	-1.08242e-11	4.99781e-23	49720.80
3.05000e-08	-1.11540e-11	5.67452e-23	3.20000e-08	-1.08506e-11	5.04495e-23	49105.05
3.06000e-08	-1.11788e-11	5.73052e-23	3.21000e-08	-1.08752e-11	5.09241e-23	48485.99
3.07000e-08	-1.12018e-11	5.78689e-23	3.22000e-08	-1.08979e-11	5.14015e-23	47859.75
3.08000e-08	-1.12230e-11	5.84362e-23	3.23000e-08	-1.09190e-11	5.18818e-23	47255.71
3.09000e-08	-1.12425e-11	5.90072e-23	3.24000e-08	-1.09384e-11	5.23653e-23	46647.26
3.10000e-08	-1.12603e-11	5.95820e-23	3.25000e-08	-1.09562e-11	5.28515e-23	46041.91
3.11000e-08	-1.12765e-11	6.01604e-23	3.26000e-08	-1.09725e-11	5.33407e-23	45440.64
3.12000e-08	-1.12913e-11	6.07425e-23	3.27000e-08	-1.09873e-11	5.38333e-23	44843.35
3.13000e-08	-1.13046e-11	6.13285e-23	3.28000e-08	-1.10006e-11	5.43287e-23	44251.9[illegible]
3.14000e-08	-1.13164e-11	6.19182e-23	3.29000e-08	-1.10125e-11	5.48271e-23	4366[illegible]
3.15000e-08	-1.13268e-11	6.25117e-23	3.30000e-08	-1.10231e-11	5.53285e-23	43083.42
3.16000e-08	-1.13358e-11	6.31090e-23	3.31000e-08	-1.10323e-11	5.58331e-23	42507.06
3.17000e-08	-1.13436e-11	6.37100e-23	3.32000e-08	-1.10403e-11	5.63407e-23	41938.20
3.18000e-08	-1.13501e-11	6.43148e-23	3.33000e-08	-1.10471e-11	5.68513e-23	41371.05
3.19000e-08	-1.13555e-11	6.49235e-23	3.34000e-08	-1.10527e-11	5.73650e-23	40811.75
3.20000e-08	-1.13596e-11	6.55360e-23	3.35000e-08	-1.10572e-11	5.78818e-23	40254.26
3.21000e-08	-1.13626e-11	6.61523e-23	3.36000e-08	-1.10606e-11	5.84017e-23	39710.82
3.22000e-08	-1.13646e-11	6.67725e-23	3.37000e-08	-1.10629e-11	5.89247e-23	39162.15
3.23000e-08	-1.13655e-11	6.73965e-23	3.38000e-08	-1.10642e-11	5.94508e-23	38624.11
3.24000e-08	-1.13654e-11	6.80244e-23	3.39000e-08	-1.10646e-11	5.99801e-23	38104.95
3.25000e-08	-1.13643e-11	6.86562e-23	3.40000e-08	-1.10639e-11	6.05124e-23	37592.1
3.26000e-08	-1.13623e-11	6.92919e-23	3.41000e-08	-1.10624e-11	6.10479e-23	37065.46
3.27000e-08	-1.13593e-11	6.99315e-23	3.42000e-08	-1.10600e-11	6.15865e-23	36555.79
3.28000e-08	-1.13555e-11	7.05751e-23	3.43000e-08	-1.10567e-11	6.21284e-23	36041
3.29000e-08	-1.13509e-11	7.12225e-23	3.44000e-08	-1.10526e-11	6.26734e-23	35553.21
3.30000e-08	-1.13454e-11	7.18740e-23	3.45000e-08	-1.10477e-11	6.32215e-23	35051.7
3.31000e-08	-1.13392e-11	7.25293e-23	3.46000e-08	-1.10421e-11	6.37729e-23	34576.49
3.32000e-08	-1.13322e-11	7.31887e-23	3.47000e-08	-1.10357e-11	6.43274e-23	34097.55
3.33000e-08	-1.13245e-11	7.38520e-23	3.48000e-08	-1.10286e-11	6.48852e-23	33624.39
3.34000e-08	-1.13161e-11	7.45194e-23	3.49000e-08	-1.10209e-11	6.54461e-23	33154.43
3.35000e-08	-1.13070e-11	7.51907e-23	3.50000e-08	-1.10124e-11	6.60103e-23	32694.19
3.36000e-08	-1.12973e-11	7.58661e-23	3.51000e-08	-1.10033e-11	6.65777e-23	32244.12
3.37000e-08	-1.12869e-11	7.65454e-23	3.52000e-08	-1.09937e-11	6.71484e-23	31790.11
3.38000e-08	-1.12759e-11	7.72289e-23	3.53000e-08	-1.09834e-11	6.77223e-23	31354.29
3.39000e-08	-1.12644e-11	7.79164e-23	3.54000e-08	-1.09726e-11	6.82995e-23	3091[illegible]
3.40000e-08	-1.12523e-11	7.86079e-23	3.55000e-08	-1.09613e-11	6.88807e-23	3048[illegible]
3.41000e-08	-1.12397e-11	7.93035e-23	3.56000e-08	-1.09494e-11	6.94637e-23	3005[illegible]
3.42000e-08	-1.12266e-11	8.00031e-23	3.57000e-08	-1.09370e-11	7.00507e-23	2964[illegible]
3.43000e-08	-1.12130e-11	8.07072e-23	3.58000e-08	-1.09242e-11	7.06410e-23	29234.75
3.44000e-08	-1.11992e-11	8.14151e-23	3.59000e-08	-1.09108e-11	7.12345e-23	28822.44
3.45000e-08	-1.11843e-11	8.21272e-23	3.60000e-08	-1.08971e-11	7.18315e-23	2842[illegible]
3.46000e-08	-1.11693e-11	8.28434e-23	3.61000e-08	-1.08829e-11	7.24314e-23	28032.56
3.47000e-08	-1.11539e-11	8.35634e-23	3.62000e-08	-1.08683e-11	7.30354e-23	2764[illegible]
3.48000e-08	-1.11381e-11	8.42884e-23	3.63000e-08	-1.08533e-11	7.36424e-23	2725[illegible]
3.49000e-08	-1.11220e-11	8.50170e-23	3.64000e-08	-1.08380e-11	7.42529e-23	26881.71
3.50000e-08	-1.11054e-11	8.57492e-23	3.65000e-08	-1.08223e-11	7.48663e-23	26505.73

TABLE X Lattice energy terms of RbCl

```
*140 PRINT R1,A1,A2,A3,A4

*RUN

```

r_1	$\frac{ne^2}{r_1}$ (ergs)	$\frac{ne^2}{r_2}$ (ergs)	B_1 (r)	B_2 (r)
3.220 [illegible]e-08	1.24[illegible]3e-11	1.20330e-11	1.[illegible]e-12	1.[illegible]e-12
3.230[illegible]e-08	1.24[illegible]e-11	1.19[illegible]3e-11	1.[illegible]e-12	1.[illegible]e-13
3.24[illegible]e-08	1.24102e-11	1.[illegible]20e-11	1.72119e-12	1.[illegible]e-12
3.25[illegible]e-08	1.23720e-11	1.1927[illegible]e-11	1.67122e-12	1.[illegible]e-12
3.260[illegible]e-08	1.23[illegible]41e-11	1.1892[illegible]e-11	1.622[illegible]e-12	1.5013[illegible]e-12

```
ready
*140 PRINT R1,Y1,Y2,Y3,Y4

*RUN

```

3.220[illegible]e-08	1.[illegible]e-12	[illegible].522[illegible]e-14	1.51100e-12	2.4[illegible]e-13
3.230[illegible]e-08	1.[illegible]44e-12	[illegible]221[illegible]e-14	1.4[illegible]84e-12	2.3[illegible]e-13
3.240[illegible]e-08	1.[illegible]e-12	[illegible].9[illegible]231e-14	1.[illegible]e-12	2.30[illegible]e-13
3.25[illegible]e-08	1.00[illegible]e-12	[illegible].65470e-14	1.38[illegible]e-12	2.23122e-13
3.260[illegible]e-08	1.[illegible]e-12	[illegible].38321e-14	1.34[illegible]e-12	2.1[illegible]e-13

```
ready
*140 PRINT R1,S1,S2

*RUN

```

3.22[illegible]e-08	2.[illegible]23	.[illegible]331[illegible]
3.23[illegible]e-08	2.[illegible]23	.[illegible]331[illegible]
3.24[illegible]e-08	2.[illegible]23	.[illegible]331[illegible]
3.25[illegible]e-08	2.[illegible]23	.[illegible]331[illegible]
3.26[illegible]e-08	2.[illegible]23	.[illegible]331[illegible]

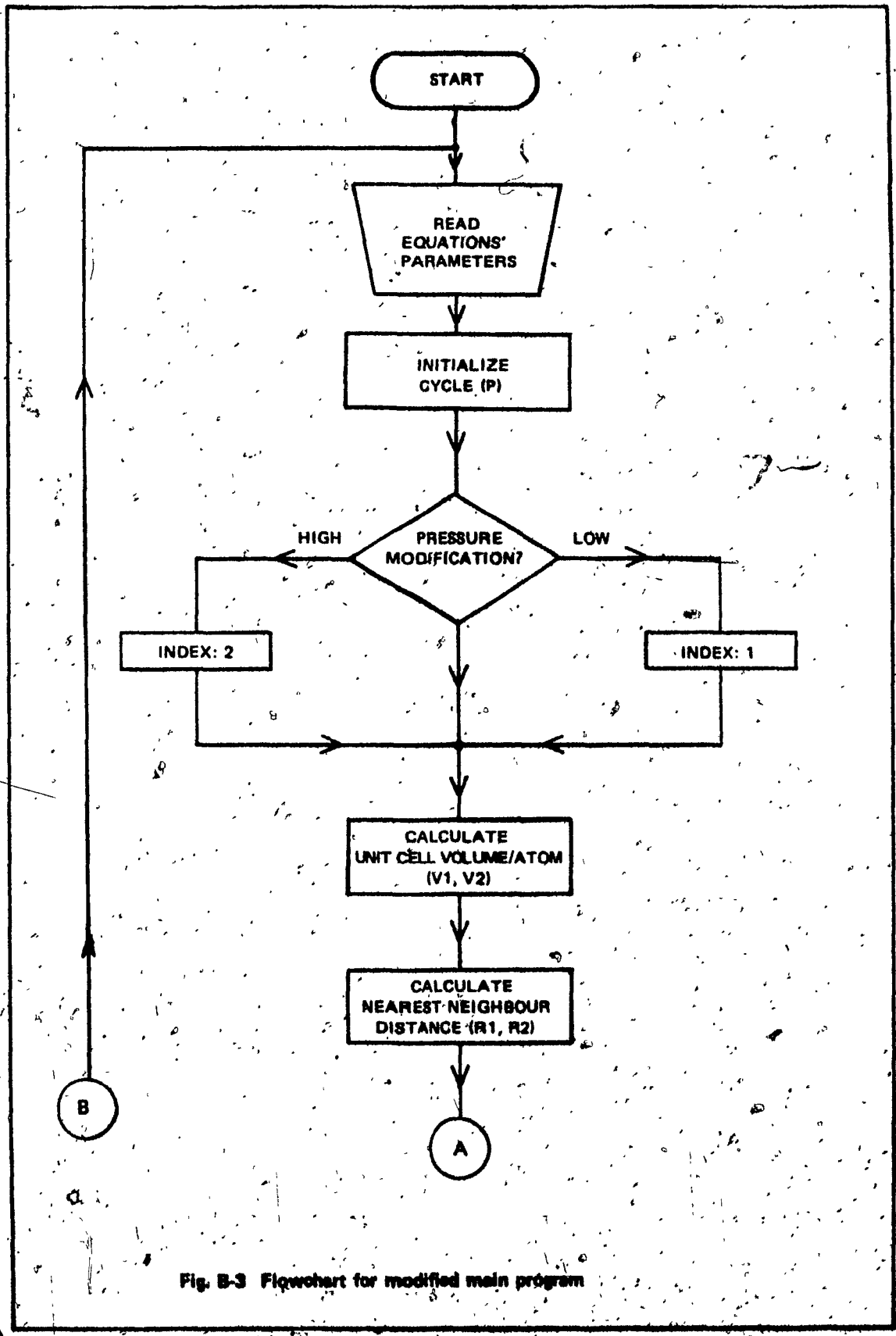

Fig. B-3 Flowchart for modified main program

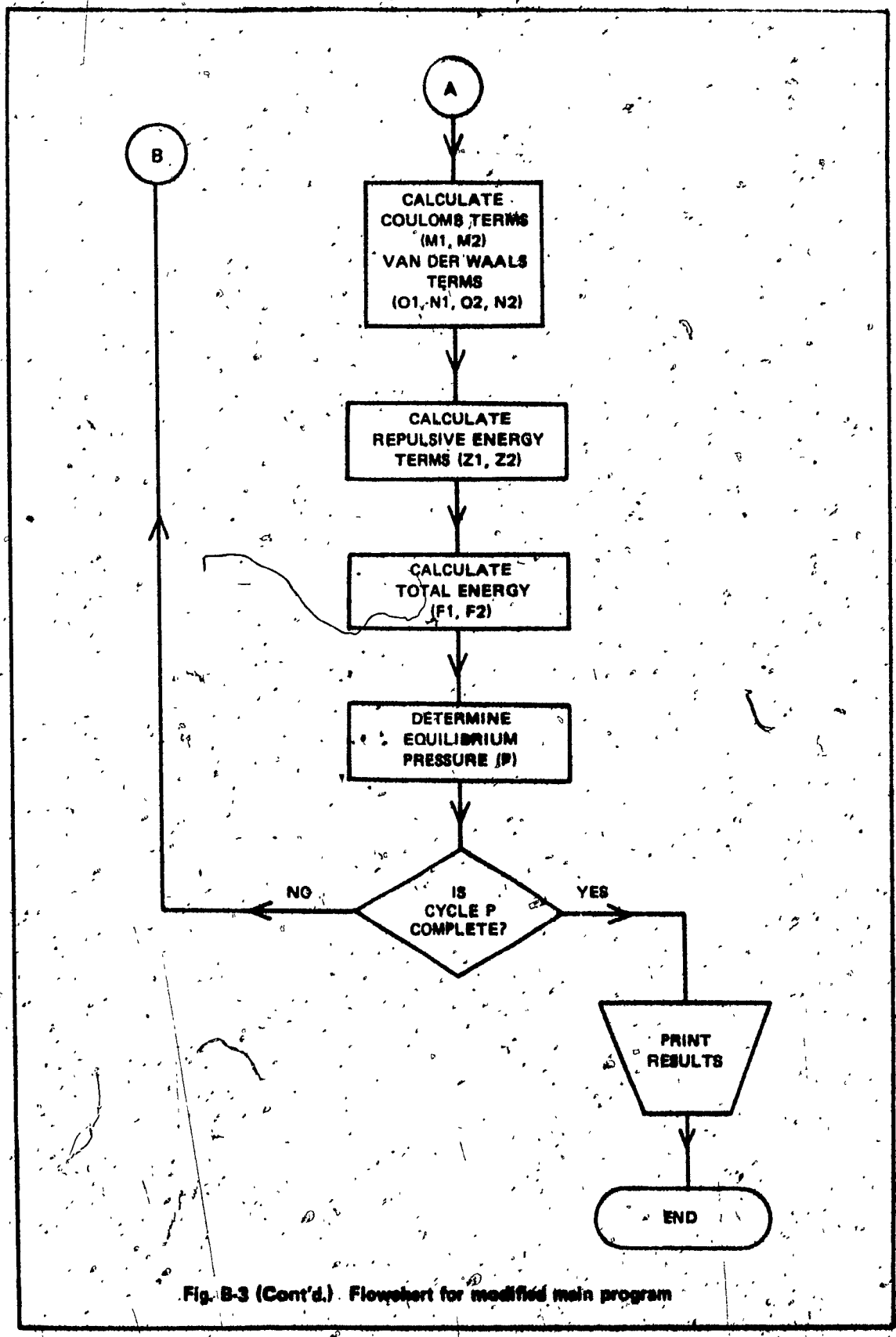

Fig. B-3 (Cont'd.) Flowchart for modified main program

```
      CALL FPARAX(1,120)
      DOUBLE PRECISION M1,I1,O1,N1,G1,G2,V1,E1,P1,Z1,Y1,Y2,S1,F1,M2,
   &  N2,I2,Y3,S2,Y4,Z2,E2,V2,P2,F2,O2
      REAL K,K1
    1 READ 10,I,J,L
   10 FORMAT(3I10)
      IF(I.EQ.0)STOP
      DO 50 IR=I,J,L
      P1=(IR/10.)*980665
      G1=VA/(1-K*P3)
      G2=V3/(1-K1*P3)
      V1=(1-K*P1)*G1
      R=(V1/2.)**(1./3.)*1E8
      M1=((A*(E**2))/R)*1E8
      O1=C/(R**6)
      N1=D/(R**8)
      I1=M1+O1+N1
      R1=R*1E-8
      Y1=B*C1*A*(EXP(((X+Z)-R1)/W))
      S1=(C2/C1)*(A3/(2.*A))*A1*(1+(C3/C2)*(EXP((-2*D1)/W)))*(EXP(D1/W))
      Y2=Y1*((S1/A1)*(EXP(-((A1-1)*R1)/W)))
      Z1=Y1+Y2
      E1=-I1+Z1
      G3=(P1/980665.)
      F1=E1+(P1*V1)
      P2=P1
      V2=(1-K1*P2)*G2
      R2=(((V2*(DSQRT(27.0D0)))/4.)**(1./3.))*1E8
      M2=((A3*(E**2))/R2)*1E8
      O2=C4/(R2**6)
      N2=D2/(R2**8)
      I2=M2+O2+N2
      R3=R2*1E-8
      Y3=B*C1*A4*(EXP(((X+Z)-R3)/W))
      S2=(C2/C1)*(A5/(2.*A4))*A2*(1+(C3/C2)*(EXP((-2*D1)/W)))*(EXP(D1/W))
      Y4=Y3*((S2/A2)*(EXP(-((A2-1)*R3)/W)))
      Z2=Y3+Y4
      E2=-I2+Z2
      G4=(P2/980665.)
      F2=E2+(P2*V2)
      P=((E2-E1)/(V1-V2))*(1.019*1E-6)
      PRINT 30,G3,F1,G4,F2
   30 FORMAT(4X,F15.2,3X,D24.14,10X,F15.2,3X,D24.14)
   50 CONTINUE
      DATA A,A1,E,C,D,B,C1,M,X,Z,W,C2,A3,C3,D1,C4,D2,A4,A5,A2,A3,K
   & ,K1,P3,V3,V4/1.7476,1.41,4.79663E-10,691E-12,960E-12,1E-12,1.,5.
   & 1.320E-8,1.475E-8,0.345E-8,0.75,12,1.25,0.155E-8,1023E-12,
   & 1470E-12,8.0,1.1547,1.7626,7.4E-12,3.7E-12,5.4E9,6.0E-23,6.362E-23/
      GO TO 1
      END
```

Fig. B-4 Modified main program

TABLE XI Total lattice energy of RbCl at low and high pressure modifications

P (kg/cm^2)	E_1 (ergs)	P (kg/cm^2)	E_2 (ergs)
33197.30	-0.92346937733197D-11	33197.30	-0.92345228121349D-11
33197.40	-0.92346864085467D-11	33197.40	-0.92345175273152D-11
33197.50	-0.92346794942285D-11	33197.50	-0.923451242317[illegible]D-11
33197.60	-0.92346723349255D-11	33197.60	-0.923450733915[illegible]D-11
33197.70	-0.92346654974734D-11	33197.70	-0.923450214422[illegible]D-11
33197.80	-0.92346580693385D-11	33197.80	-0.9234596[illegible]D-11
33197.90	-0.92346507051153D-11	33197.90	-0.92345915[illegible]D-11
33198.00	-0.92346437933541D-11	33198.00	-0.923458551224[illegible]D-11
33198.10	-0.92346364341514D-11	33198.10	-0.92345813627421D-11
33198.20	-0.92346295293927D-11	33198.20	-0.92345752183230D-11
33198.30	-0.92346221545209D-11	33198.30	-0.923457110[illegible]D-11
33198.40	-0.92346152597159D-11	33198.40	-0.92345[illegible]D-11
33198.50	-0.92346079934169D-11	33198.50	-0.92345[illegible]D-11
33198.60	-0.92346010150725D-11	33198.60	-0.92345552[illegible]D-11
33198.70	-0.92345941102215D-11	33198.70	-0.92345500745725D-11
33198.80	-0.92345870745315D-11	33198.80	-0.92345448[illegible]D-11
33198.90	-0.92345797448335D-11	33198.90	-0.92345398[illegible]D-11
33199.00	-0.92345724694957D-11	33199.00	-0.92345347[illegible]D-11
33199.10	-0.92345655637120D-11	33199.10	-0.923452[illegible]5234D-11
33199.20	-0.92345583199373D-11	33199.20	-0.92345241[illegible]D-11
33199.30	-0.92345512938442D-11	33199.30	-0.923451[illegible]D-11
33199.40	-0.92345443939545D-11	33199.40	-0.923451380925[illegible]D-11
33199.50	-0.92345370347113D-11	33199.50	-0.92345085[illegible]D-11
33199.60	-0.92345296643144D-11	33199.60	-0.92345034803[illegible]D-11
33199.70	-0.92345227634411D-11	33199.70	-0.92344983125[illegible]D-11
33199.80	-0.92345153998423D-11	33199.80	-0.923449314685[illegible]D-11
33199.90	-0.92345083493443D-11	33199.90	-0.92344879[illegible]D-11
33200.00	-0.92345011276095D-11	33200.00	-0.92344825940[illegible]D-11

332000 332200 1

P (kg/cm^2)	E_1 (ergs)	P (kg/cm^2)	E_2 (ergs)
33200.00	-0.92345011276095D-11	33200.00	-0.92344826947[illegible]D-11
33200.10	-0.92344942155373D-11	33200.10	-0.92344775093185D-11
33200.20	-0.92344865577283D-11	33200.20	-0.92344723544[illegible]D-11
33200.30	-0.92344799734995D-11	33200.30	-0.92344572052[illegible]D-11
33200.40	-0.92344727773770D-11	33200.40	-0.92344620[illegible]D-11
33200.50	-0.92344655412915D-11	33200.50	-0.92344568[illegible]D-11
33200.60	-0.92344585337309D-11	33200.60	-0.92344517213[illegible]D-11
33200.70	-0.92344511428591D-11	33200.70	-0.923444465423[illegible]D-11
33200.80	-0.92344442628212D-11	33200.80	-0.92344413991[illegible]D-11
33200.90	-0.92344369970585D-11	33200.90	-0.923443521471[illegible]D-11
33201.00	-0.92344299926558D-11	33201.00	-0.92344310[illegible]D-11
33201.10	-0.92344226291617D-11	33201.10	-0.92344257[illegible]D-11
33201.20	-0.92344157317919D-11	33201.20	-0.92344205[illegible]D-11
33201.30	-0.92344088261117D-11	33201.30	-0.923441542237[illegible]D-11
33201.40	-0.92344014615449D-11	33201.40	-0.92344102[illegible]D-11
33201.50	-0.92343945508659D-11	33201.50	-0.92344050[illegible]D-11
33201.60	-0.92343871857577D-11	33201.60	-0.92343999[illegible]D-11
33201.70	-0.92343802772539D-11	33201.70	-0.92343941731[illegible]D-11
33201.80	-0.92343729146769D-11	33201.80	-0.923433891235[illegible]D-11
33201.90	-0.92343660095277D-11	33201.90	-0.92343334145[illegible]D-11
33202.00	-0.92343586544237D-11	33202.00	-0.923437[illegible]D-11
33202.10	-0.92343517392314D-11	33202.10	-0.92343734055[illegible]D-11
33202.20	-0.92343443731948D-11	33202.20	-0.923435[illegible]D-11
33202.30	-0.92343374944048D-11	33202.30	-0.92343533527[illegible]D-11
33202.40	-0.92343301027245D-11	33202.40	-0.923435[illegible]D-11
33202.50	-0.92343232249585D-11	33202.50	-0.923435314432[illegible]D-11
33202.60	-0.92343159579207D-11	33202.60	-0.92343347[illegible]D-11
33202.70	-0.92343084952755D-11	33202.70	-0.92343427201022D-11
33202.80	-0.92343015840599D-11	33202.80	-0.92343375413[illegible]D-11
33202.90	-0.92342945736252D-11	33202.90	-0.92343323[illegible]D-11
33203.00	-0.92342877311698D-11	33203.00	-0.92343272072[illegible]D-11
33203.10	-0.92342804053471D-11	33203.10	-0.9234312[illegible]D-11
33203.20	-0.92342732367132D-11	33203.20	-0.9234316714111[illegible]D-11
33203.30	-0.92342659708895D-11	33203.30	-0.92343111057[illegible]D-11
33203.40	-0.92342589565313D-11	33203.40	-0.923430041261951D-11
33203.50	-0.92342516005503D-11	33203.50	-0.92343012602170D-11

APPENDIX C

COMPUTERIZED PROCEDURE - $HgSe_xTe_{(1-x)}$

Description

The calculation of the theoretical transition pressures of the mercury chalcogenides was based on the program developed for the the alkali halides, as shown in Appendix B.

The main program, with the necessary modifications, was here used. The modifications are necessary to account for the difference in nature of the mercury chalcogenides as compared to the alkali halides. The program is shown in Fig. C-1.

The theoretically calculated transition pressures, for the $HgSe_xTe_{(1-x)}$ compounds and their alloys are shown in the computer printouts in the Tables XII - XIV. The numerical values corresponding to these pressures are those of the middle row for each case.

The dominance of the Coulomb energy term over the repulsive energy term is evident from the values obtained for both the low pressure phase (first two columns) and the high pressure phase modifications (next two columns). These values are as in the Tables XV - XVII.

```
 5      MARGIN#0,120
 10   FOR R=2.62 TO 2.64 STEP 0.01
 15     READ A,A1,E,B,C1,M,N,C2,M3,C3,M4,M5,A3,A2
 16     READ X,Z,D1
 20     LET M1=((A*(E^2))/R)*1E8
 35     LET I1=M1
 40     LET R1=R*1E-8
 45     LET Y1=B*C1*M*(EXP(((X+Z)-R1)/N))
 50     LET S1=(C2/C1)*(M3/(2*M))*A1*(1+(C3/C2)*(EXP((-2*D1)/N)))*(EXP(D1/N))
 55     LET Y2=Y1*((S1/A1)*(EXP(-((A1-1)*R1)/N)))
 60     LET Z1=Y1+Y2
 65     LET E1=-I1+Z1
 70     LET V1=3.075*(R1^3)
 75     LET R2=R-0.2
 80     LET M2=((A3*(E^2))/R2)*1E8
 95     LET I2=M2
 100    LET R3=R2*1E-8
 105    LET Y3=B*C1*M4*(EXP(((X+Z)-R3)/N))
 110  LET S2=(C2/C1)*(M5/(2*M4))*A2*(1+(C3/C2)*(EXP((-2*D1)/N)))*(EXP(D1/N))
 115    LET Y4=Y3*((S2/A2)*(EXP(-((A2-1)*R3)/N)))
 120    LET Z2=Y3+Y4
 125    LET E2=-I2+Z2
 126    LET R4=R2
 129  LET G=(((SQR((R4^2-3.3)/0.130))*1E-8)^3)
 130    LET V2=0.042*G
 135  LET P=((E2-E1)/(V1-V2))*(1.019*1E-6)
 140  PRINT E1,E2,V1,V2,P
 145    RESTORE
 150    NEXT R
 155    DATA 1.0381,1.3,4.79608E-10,1E-12,0.861,4
 160    DATA 0.596E-8,0.5,12,1.22,2,2,1.4,1.56
 161    DATA 1.392E-8,1.072E-8,0.320E-8
 170    STOP

ready.
*
```

Fig. C-1 Program for the calculation of the theoretical transition pressures of $HgSe_x Te_{(1-x)}$

TABLE XII Calculated transition pressures of $HgS_xTe_{(1-x)}$

E_1 (ergs)	E_2 (ergs)	V_1 (cm^3)	V_2 (cm^3)	P (kg/cm^2)
-1.12803e-11	-1.12826e-11	5.53030e-23	5.23202e-23	-829.6059
-1.12820e-11	-1.12633e-11	5.59387e-23	5.38162e-23	8964.476
-1.12830e-11	-1.12437e-11	5.65792e-23	5.53324e-23	32122.71

(a) HgS_e

```
ready
*TAPE

READY
 10    FOR R=2.603 TO 2.665 STEP 0.001
 75    LET R2=R-0.24
 129   LET G=(((SQR((R4^2-3.32)/0.129))*1E-8)^3)
 130   LET V2=0.632*G
 100   DATA 0.566E-8,0.5,12,1.22,2,2,1.4,1.55
 101   DATA 1.406E-8,1.117E-8,0.289E-8
*RUN
```

-1.10853e-11	-1.10619e-11	5.80709e-23	5.55751e-23	9547.704
-1.10858e-11	-1.10605e-11	5.81363e-23	5.57335e-23	10721.07
-1.10863e-11	-1.10592e-11	5.82018e-23	5.58922e-23	11987.81

(b) $HgS_{e_{0.8}}Te_{0.2}$

```
ready
*
```

TABLE XIII Calculated transition pressures of $HgSe_x\ Te_{(1-x)}$

```
TAPE
READY
10      FOR R=2.697 TO 2.699 STEP 0.001
15      LET R2=R-0.28
129     LET G=(((50R((R4^2-3.4)/0.12))*1E-8)^(_3)
130     LET V2=0.622*G
1000    DATA 0.5476E-8,0.5,12,1.22,2,2,1.4,1.54
1010    DATA 1.421E-8,1.164E-8,0.257E-8
*RUN
```

E_1 (ergs)	E_2 (ergs)	V_1 (cm^3)	V_2 (cm^3)	P (kg/cm^2)
-1.08244e-11	-1.07909e-11	6.03237e-23	5.70962e-23	10603.31
-1.08254e-11	-1.07902e-11	6.03908e-23	5.72659e-23	11490.41
-1.08264e-11	-1.07895e-11	6.04580e-23	5.74358e-23	12437.28

(c) $HgSe_{0.6}\ Te_{0.4}$

```
ready
*TAPE
READY
10      FOR R=2.731 TO 2.733 STEP 0.001
15      LET R2=R-0.32
129     LET G=(((50R((R4^2-3.43)/0.1143))*1E-8)^3)
130     LET V2=0.612*G
1000    DATA 0.5380E-8,0.5,12,1.22,2,2,1.4,1.54
1010    DATA 1.436E-8,1.211E-8,0.225E-8
*RUN
```

-1.05252e-11	-1.04753e-11	5.20340e-23	5.32568e-23	11003.22
-1.05260e-11	-1.04754e-11	5.21028e-23	5.84337e-23	12220.47
-1.05268e-11	-1.04754e-11	5.21717e-23	5.86109e-23	12481.93

(d) $HgSe_{0.4}\ Te_{0.6}$

```
ready
*
```

TABLE XIV Calculated transition pressures of HgS_{e_x} $Te_{(1-x)}$

```
TAPE

READY
10      FOR R=2.705 TO 2.707 STEP 0.001
75      LET R2=R-0.34
129     LET G=(((SQR((R4^2-3.47)/0.1126))*1E-8)^3)
130     LET V2=0.002*G
160     LET___DATA 0.539E-8,0.5,12,1.22,2,2,1.4,1.53
101     DATA 1.451E-8,1.258E-8,0.193E-8
*RUN
```

E_1 (ergs)	E_2 (ergs)	V_1 (cm^3)	V_2 (cm^3)	P (kg/cm^2)
-1.01920e-11	-1.01218e-11	6.50026e-23	5.96325e-23	13309.79
-1.01938e-11	-1.01225e-11	6.50731e-23	5.98126e-23	13821.78
-1.01950e-11	-1.01231e-11	6.51437e-23	5.99930e-23	14355.62

(e) $HgS_{e_{0.2}}$ $Te_{0.8}$

```
ready
*TAPE

READY
10      FOR R=2.79 TO 2.81 STEP 0.01
75      LET R2=R-0.39
129     LET G=(((SQR((R4^2-3.53)/0.11))*1E-8)^3)
130     LET V2=0.59*G
100     DATA 0.54E-8,0.5,12,1.22,2,2,1.4,1.53
101     DATA 1.400E-8,1.307E-8,0.159E-8
*RUN
```

-9.81715e-12	-9.73105e-12	6.07817e-23	5.91870e-23	11553.09
-9.84067e-12	-9.74402e-12	6.75024e-23	6.10175e-23	15186.55
-9.86310e-12	-9.75614e-12	6.82282e-23	6.28735e-23	20355.48

(f) Hg Te

```
ready
*
```

TABLE XV Lattice energy terms of $HgS_{e_x}T_{e_{(1-x)}}$

```
ready
*140  PRINT M1,Z1,M2,Z2,P

*RUN
```

$\frac{\alpha e^2}{r_1}$ (ergs)	B_1 (r) (ergs)	$\frac{\alpha e^2}{r_2}$ (ergs)	B_2 (r) (ergs)	P (kg/cm^2)
1.43654e-11	3.10502e-12	1.33105e-11	2.02173e-12	-829.0659
1.43307e-11	3.04807e-12	1.32557e-11	1.99240e-12	8904.470
1.42704e-11	2.99337e-12	1.32014e-11	1.95769e-12	32122.71

(a) HgSe

```
ready
*TAPE

READY
10    FOR R=2.663 TO 2.605 STEP 0.001 .
75    LET R2=R-0.24
129   LET G=(((SQR((R4^2-3.32)/0.129))*1E-8)^3)
130   LET V2=0.032*G
100   DATA 0.566E-3,0.5,12,1.22,2,2,1.4,1.55
101   DATA 1.406E-8,1.117E-8,0.289E-8
*RUN
```

1.41531e-11	3.00776e-12	1.32940e-11	2.23210e-12	9547.704
1.41470e-11	3.00194e-12	1.32885e-11	2.22799e-12	10721.07
1.41425e-11	3.00512e-12	1.32830e-11	2.22389e-12	11987.81

(b) $HgS_{e_{0.8}}T_{e_{0.2}}$

```
ready
*
```

TABLE XVI Lattice energy terms of $HgS_{e_x} T_{e_{(1-x)}}$

```
TAPE

READY
*TAPE

READY
10 .   FOR R=2.097 TO 2.099 STEP 0.001
70     LET R2=R-0.28
129    LET G=(((SQR((R4^2-3.4)/0.12))*1E-8)^#_3)
130    LET V2=0.622*G
100    DATA 0.5476E-8,0.5,12,1.22,2,2,1.4,1.54
101    DATA 1.421E-8,1.104E-8,0.257E-8
*RUN
```

$\frac{\alpha e^2}{r_1}$ (ergs)	B_1 (r) (ergs)	$\frac{\alpha e^2}{r_2}$ (ergs)	B_2 (r) (ergs)	P (kg/cm^2)
1.39747e-11	3.15021e-12	1.33270e-11	2.53615e-12	10603.31
1.39095e-11	3.14406e-12	1.33215e-11	2.53133e-12	11490.41
1.39043e-11	3.13794e-12	1.33160e-11	2.52652e-12	12437.28

(c) $HgS_{e_{0.6}} T_{e_{0.4}}$

```
ready
*TAPE

READY
10 .   FOR R=2.731 TO 2.733 STEP 0.001
70     LET R2=R-0.32
129    LET G=(((SQR((R4^2-3.43)/0.1143))*1E-8)^3)
130    LET V2=0.612*G
100    DATA 0.5380E-8,0.5,12,1.22,2,2,1.4,1.54
101    DATA 1.430E-8,1.211E-8,0.225E-8
*RUN
```

1.38007e-11	3.27548e-12	1.33602e-11	2.88483e-12	11003.22
1.37950e-11	3.26902e-12	1.33540e-11	2.87927e-12	12220.47
1.37906e-11	3.26258e-12	1.33491e-11	2.87371e-12	12881.93

(d) $HgS_{e_{0.4}} T_{e_{0.6}}$

```
ready
*
```

TABLE XVII Lattice energy terms of $HgS_{e_x}T_{e_{(1-x)}}$

```
TAPE

READY
10      FOR R=2.765 TO 2.767 STEP 0.001
75      LET R2=R-0.34
129     LET G=(((SQR((R4^2-3.47)/0.1126))*1E-8)^3)
130     LET V2=0.0062*G
100     LET___DATA 0.539E-8,0.5,12,1.22,2,2,1.4,1.53
101     DATA 1.451E-8,1.258E-8,0.193E-8
*RUN
```

$\frac{\alpha e^2}{r_1}$ (ergs)	B_1 (r) (ergs)	$\frac{\alpha e^2}{r_2}$ (ergs)	B_2 (r) (ergs)	P (kg/cm^2)
1.36310e-11	3.43898e-12	1.32830e-11	3.16121e-12	13309.79
1.36260e-11	3.43222e-12	1.32776e-11	3.15511e-12	13621.78
1.36211e-11	3.42547e-12	1.32721e-11	3.14902e-12	14355.62

(e) $HgSe_{0.2}Te_{0.8}$

```
ready
*TAPE

READY
10      FOR R=2.79 TO 2.81 STEP 0.01
75      LET R2=R-0.30
129     LET G=(((SQR((R4^2-3.53)/0.11))*1E-8)^3)
130     LET V2=0.59*G
100     DATA 0.54E-8,0.5,12,1.22,2,2,1.4,1.53
101     DATA 1.466E-8,1.307E-8,0.159E-8
*RUN
```

1.35086e-11	3.69108e-12	1.32557e-11	3.52407e-12	11553.09
1.34660e-11	3.61991e-12	1.32014e-11	3.45737e-12	15180.55
1.34127e-11	3.54956e-12	1.31475e-11	3.39137e-12	20355.46

(f) $Hg\,T_e$

```
ready
*
```